

ADA081902



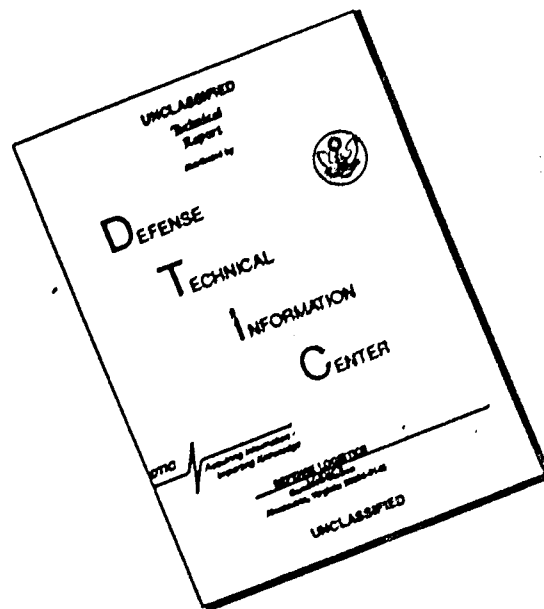
RECEIVED
LIBRARY OF CONGRESS

1981
JAN 15 1981
LIBRARY OF CONGRESS
JAN 15 1981

U.S. DEPARTMENT OF COMMERCE

OFFICE OF ECONOMIC AFFAIRS
WASHINGTON, D.C. 20540
JAN 15 1981

DISCLAIMER NOTICE



THIS DOCUMENT IS BEST QUALITY AVAILABLE. THE COPY FURNISHED TO DTIC CONTAINED A SIGNIFICANT NUMBER OF PAGES WHICH DO NOT REPRODUCE LEGIBLY.

2-D FLOW NUMERICAL SOLUTION FOR
AIRFOIL AND HOVERCRAFT IN GROUND EFFECT

THESIS

AFIT/GAE/AA/78D-6 ✓

Itzhak Dvir
Maj IAF

Approved for public release; distribution unlimited.

14

AFIT/GAE/AA/78D-6

6

2-D FLOW NUMERICAL SOLUTION FOR
AIRFOIL AND HOVERCRAFT IN GROUND EFFECT

9

Master's THESIS

Presented to the Faculty of the School of Engineering
of the Air Force Institute of Technology
Air University

in Partial Fulfillment of the
Requirements for the Degree of
Master of Science

by

10

Itzhak Dvir B.S.
Maj IAF

Graduate Aeronautical Engineering

11

Dec 1978

Accession For	
NTIS	General
DDI	TAR
Unannounced	
Continued	
A	

PII Redacted

012225

ACKNOWLEDGMENTS

I wish to express my sincere appreciation to Dr J. Shea who guided me in my study. This study would not have been possible without his assistance.

Also, I wish to thank my wife, Zhava, and my family whose understanding and patience let me complete this thesis.

Itzhak Dvir

TABLE OF CONTENTS

	<u>Page</u>
ACKNOWLEDGEMENTS	ii
LIST OF FIGURES	v
LIST OF TABLES	vii
LIST OF SYMBOLS	viii
ABSTRACT	x
I. INTRODUCTION	1
Background	1
Purpose of This Study	2
Procedure	2
Specific Problems Addressed	3
II. FINITE SINGULARITY METHOD	5
Thin Airfoil Theory	5
Method Description	6
Flat Plate in Ground Effect	8
Results	9
III. COORDINATE TRANSFORMATION	17
Mathematical Development	17
Coordinate System Control	19
Difference Equations	20
Transformation Properties	20
Applications	21
IV. STREAM FUNCTION SOLUTION	26
Differential Equation and Aerodynamic Coefficients	26
Difference Equations	27
Applications	28
V. AIRFOIL STREAM FUNCTION SOLUTION	32
Airfoil Type	32
Kutta Condition	32
Airfoil in Free Stream	34
Airfoil in Ground Effect	45
Summary	46

TABLE OF CONTENTS
(Continued)

	<u>Page</u>
VI. HOVERCRAFT STREAM FUNCTION SOLUTION	53
Hovercraft Model	53
Multi-Valued Stream Function	57
Vorticity	59
Pressure Derivation	62
Summary	62
VII. CONCLUSIONS	64
BIBLIOGRAPHY.	65
APPENDIX A: Computer Programs Description	66
APPENDIX B: Chordwise C_p Variation for Flat Plate	71
VITA.	73

LIST OF FIGURES

<u>Figure</u>	<u>Page</u>
1. Finite Singularity Method	7
2. Flat Plate in Ground Effect	7
3. Lift Coefficient vs. Angle of Attack. Ground Distance as a Parameter (Finite Singularity Method)	11
4. Lift Coefficient vs. Ground Distance. Angle of Attack as a Parameter (Finite Singularity Method)	12
5. Quarter Chord Moment Coefficient vs. Angle of Attack. Ground Distance as a Parameter (Finite Singularity Method)	13
6. Quarter Chord Moment Coefficient vs. Ground Distance. Angle of Attack as a Parameter (Finite Singularity Method)	14
7. Field Transformation Single Body	18
8. Body-Fitted Coordinate System for a Cylinder in a Circular Outer Boundary (Entire Region)	23
9. Body-Fitted Coordinate System for a Cylinder in a Circular Outer Boundary. No Attraction of Coordinates ($P = Q = 0$). . .	24
10. Body-Fitted Coordinate System for a Cylinder in a Circular Outer Boundary. Attraction of Constant n Coordinates . . .	25
11. Pressure Coefficient on a Cylinder vs. Nondimensionalized Diameter in Free Stream Direction	30
12. Stream Function Contour Plot for Cylinder in Free Stream. .	31
13. Kutta Condition Check Scheme	33
14. Body-Fitted Coordinate System for Airfoil in Free Stream. .	35
15. Body-Fitted Coordinate System for Airfoil in Free Stream, Partial Region	36
16. Stream Function Contour Plot for Airfoil in 10° Angle of Attack in Free Stream	37
17. Pressure Coefficient vs. Nondimensionalized Chord Length in Free Stream Direction (Typical for Thin Airfoil)	42

LIST OF FIGURES

(Continued)

<u>Figure</u>		<u>Page</u>
18.	Free Stream Lift Coefficient vs. Angle of Attack	43
19.	Body-Fitted Coordinate System for Airfoil in Ground Effect	47
20.	Body-Fitted Coordinate System for Airfoil in Ground Effect, Partial Region	48
21.	Lift Coefficient vs. Ground Distance. Angle of Attack as Parameter (Finite Difference Method)	49
22.	Quarter Chord Moment Coefficient vs. Ground Distance. Angle of Attack as a Parameter (Finite Difference Method).	50
23.	Ground Velocity vs. Nondimensionalized Chord Length in Free Stream Direction	51
24.	Hovercraft Model	53
25.	Body Fitted Coordinate System for Hovercraft in Ground Effect	54
26.	Stream Function Contour Plot for Hovercraft, Potential Flow Solution	58
27.	Jet Velocity Profile	59
28.	Stream Function Contour Plot for Hovercraft, Vorticity in Jet Edges	61
B-1.	Graphic Presentation of Table B-1	72

LIST OF TABLES

<u>Table</u>		<u>Page</u>
1.	Lift Coefficient as Function of Angle of Attack and Ground Distance. Finite Singularity Method	15
2.	Quarter Chord Moment Coefficient as Function of Angle of Attack and Ground Distance. Finite Singularity Method. . .	16
3.	Numerical Data for an Airfoil in 10° Angle of Attack. . . .	38
4.	Calculated Aerodynamic Coefficients for 10° Angle of Attack for Different Airfoil Grid Point Distribution	40
5.	Aerodynamic Coefficients for Free Stream as Function of Angle of Attack. Finite Difference Method	44
6.	Aerodynamic Coefficients in Ground Effect as Function of Ground Distance and Angle of Attack. Finite Difference Method	44
7.	Numerical Data for Rectangular Outer Boundary for Airfoil in Ground Effect	52
8.	Numerical Data for a Hovercraft Model	55
9.	Numerical Data for Outer Boundary for Hovercraft	56
B-1.	Percent of C_L vs. Nondimensional Chord Measured from Leading Edge.	72

LIST OF SYMBOLS

- a - ground distance
- A - coefficients matrix (Finite Singularity method)
- c - chord
- C_l - lift coefficient
- C_m - moment coefficient
- C_p - pressure coefficient
- F - airfoil contour equation
- J - transformation Jacobian
- L - jet width
- N - number of elements
- p - transformation control function
- P - pressure
- Q - transformation control function
- t - time
- U - jet velocity
- U_0 - free stream velocity
- V - velocity
- X - coordinate
- X_0 - moment center
- Y - coordinate
- Y_a - Camber line ordinate
- α - coordinate transformation parameter
- α - angle of attack

LIST OF SYMBOLS
(continued)

- β - coordinate transformation parameter
- γ - coordinate transformation parameter
- γ - vortex strength/unit length
- Γ - finite vortex strength
- ν - kinematic viscosity
- ξ - transformed plane coordinate
- η - transformed plane coordinate
- ϕ - potential function
- ψ - stream function
- σ - coordinate transformation parameter
- τ - coordinate transformation parameter
- ω - vorticity

Subscripts

- i, I - row designator
- j, J - column designator
- L.E. - leading edge
- T.E. - trailing edge

Superscripts

- n - time level

ABSTRACT

A proposal has been made to compute a 2-D numerical solution to the stream function - vorticity equation to analyze the flow field, both of an airfoil in ground effect and of an air cushion vehicle of arbitrary geometry supported by peripheral jets. This report is an investigation of both problems. Finite difference solutions of the stream function-vorticity equation are computed on a body fitted coordinate system. The Laplace equation for streamlines around an airfoil in ground effect is solved, and results are compared to an analytic finite singularity solution. Comparison of C_L and $C_{ma.c.}$ at varying angles of attack and ground distance indicate good agreement. The finite difference method is found to be sensitive to grid point distribution about the leading edge, for which a criterion is established. Since an air cushion vehicle acts as a flow source within the field, the finite difference expression is modified to accommodate a branch cut. The presence of vorticity is essential to definition of the peripheral jets. The vorticity distribution, derived from arbitrary velocity distribution at jet outlets and assumed to be constant along streamlines, leads to a stable solution of the stream function-vorticity equation.

2-D FLOW NUMERICAL SOLUTION FOR AIRFOIL AND HOVERCRAFT IN GROUND EFFECT

I. INTRODUCTION

Background

The Air Force Flight Dynamics Laboratory is currently investigating the feasibility of designing a high performance aircraft with air cushioned wings instead of standard landing gear to achieve a take-off and landing capability on rough and bomb-damaged runways. The wing air cushion is to be generated by a peripheral jet. Investigating the behavior of such a design is a complicated fluid mechanics problem that combines air cushion dynamics with a wing in ground effect. Current methods for airfoil flow field solution range from simple potential flow solutions to viscous, compressible Navier-Stokes solutions. Air cushion flow fields are determined through experimental techniques. Current air cushion analysis (Ref 3, 7) is based upon assuming a simple jet geometry to enable integration of pressure gradients. In the commonly used exponential theory jet streamlines with a constant radius of curvature are assumed, and pressure gradients across streamlines supply the centripital acceleration. These methods provide reasonable results for symmetric cases only. Improved flow analysis of air cushion dynamics would diminish the need to evaluate design parameters exclusively through expensive experiments. A proposed approach is to determine the flow field for an air cushioned airfoil by using 2-D finite difference solution to the stream function-vorticity equations.

Purpose of This Study

The general purpose is to obtain a generally applicable method for solution of air cushioned wing flow field. In particular, a 2-D flow field solution by using the stream function-vorticity equations is proposed. This study is a small scaled feasibility study to the proposed solution and includes two separate aspects of the problem. The first aspect is investigating the behavior of a finite difference numerical solution for an airfoil in ground effect and comparing the results to those obtained by an independent method. The second aspect is to solve a symmetric case of air cushion vehicle with peripheral jet and obtain a physically reasonable flow field.

Procedure

As mentioned the flow fields in this study are solved by using the stream function-vorticity formulation. Use of the stream function guarantees conservation of mass. The general incompressible vorticity equation that is derived from momentum equations has the form.

$$\frac{D\vec{\omega}}{Dt} = \frac{\partial \vec{\omega}}{\partial t} + \vec{V} \cdot \nabla \omega = \nu \cdot \nabla^2 \omega \quad (1)$$

Equation (1) indicates that in the absence of diffusion the vorticity must be constant along streamlines, in which case equation (1) can be rewritten in stream function formulation for planar flow as

$$\nabla^2 \psi = -\omega(\psi) \quad (2)$$

A tacit assumption throughout the study is that neither the initial distribution of vorticity in the peripheral jet nor the vorticity transport has a critical impact on pressure distribution under the vehicle (both

points must be checked by an additional feasibility study). In summary, the vorticity is determined from an arbitrary assumed velocity distribution across the peripheral jet outlets in the air cushion case. For the case of the airfoil in ground effect the vorticity is set to zero.

The numerical formulation consists of generation of body fitted coordinate system by solving Poisson equations for transformed coordinates (ξ, η) as a function of physical coordinates (x, y) . Free parameters in grid generation equations as well as freedom in the selection of boundary points location allow the manipulation of the physical grid to a configuration which provides enhanced resolution where it is needed. The stream function-vorticity equations and the body fitted coordinate system equations are both transformed to the (ξ, η) plane and solved by SOR finite difference techniques.

Specific Problems Addressed

1. Cylinder in uniform potential flow

This case is solved to verify both the body fitted coordinate system generation and the potential flow stream function solution by comparison with well known analytical results.

2. Airfoil in free stream and ground effect

The 2-D flow field numerical solution is used even though it is realized that some important aspects of wing in ground effect are related to 3-D analysis, such as the dramatic decrease in induced drag and large differences in handling qualities. The airfoil flow field is analyzed with both a finite difference method and a finite singularity method. Lift and quarter chord moment coefficients variation with angle of attack and ground distance are derived by both methods and compared.

3. Air cushion device with peripheral jets

Introduction of branch cut to relieve multi-valued stream function from fluid source within the vehicle. To obtain a well defined jet, vorticity is introduced into shear layers at the edges of the peripheral jets and assumed to remain constant along each streamline.

II. FINITE SINGULARITY METHOD

In this study, the airfoil in ground effect is solved for an inviscid incompressible flow using a finite difference method. This chapter describes an airfoil in ground effect solution using a finite singularity method which establishes a comparison standard for the finite difference solution.

Thin Airfoil Theory

The problem of calculating the flow field and the aerodynamic properties of an arbitrary airfoil with no restriction as to its thickness, camber, or angle of attack, is complex in practice. Thin airfoil theory provides simplification of the mathematical problem with a rather wide applicability. In thin airfoil theory the flow around the airfoil is represented by a sheet of vortices lying along the camber line. The perturbed flow field is determined by the following (Ref 1):

1. Differential equation

$$\nabla^2 \phi = \frac{\partial^2 \phi}{\partial x^2} + \frac{\partial^2 \phi}{\partial y^2} = 0 \quad (3)$$

2. Boundary conditions

$$(U_0 + \nabla \phi) \cdot \nabla F = 0 \text{ on airfoil} \quad (4)$$

$$\nabla \phi \rightarrow 0 \quad \text{at infinity} \quad (5)$$

3. Kutta condition

The velocity is finite and continuous at the trailing edge.

Once the airfoil shape is replaced by a sheet of vorticity of strength $\gamma(x)$ at the camber line and thin airfoil assumptions are applied, the mathematical problem reduces to one singular integral equation.

$$U_0 \frac{d\gamma_a}{dx} = -\frac{1}{2\pi} \int_{-c/2}^{c/2} \frac{\gamma(\xi)}{x-\xi} d\xi \quad (6)$$

Solution of the integral equation, to determine $\gamma(x)$, can be done by the following techniques:

1. Sohngen integral inversion
2. Prandtl Glauert transformation
3. Finite singularity method

Given the vorticity distribution γ along the camber line (or along the x-axis), the lift and moment coefficients are easily found by integration.

$$C_l = \frac{2}{V_0 c} \int_{-c/2}^{c/2} \gamma(x) dx \quad (7)$$

$$C_{m_{x_0}} = \frac{2}{V_0 c^2} \int_{-c/2}^{c/2} (x_0 - x) \cdot \gamma(x) dx \quad (8)$$

The rest of this chapter deals with finite singularity solution for a flat plate in ground effect. The solution provides $\gamma(x)$, C_l , C_m as function of ground distance and angle of attack.

Method Description

The finite singularity method is an approximate numerical method to solve the integral equation (6). A finite number of point vortices is obtained by solving a set of algebraic equations, which is a very convenient computational formulation (Ref 2).

The airfoil is divided into N elements (Fig 1). Increasing N improves the accuracy, but usually ten elements are enough. A vortex of

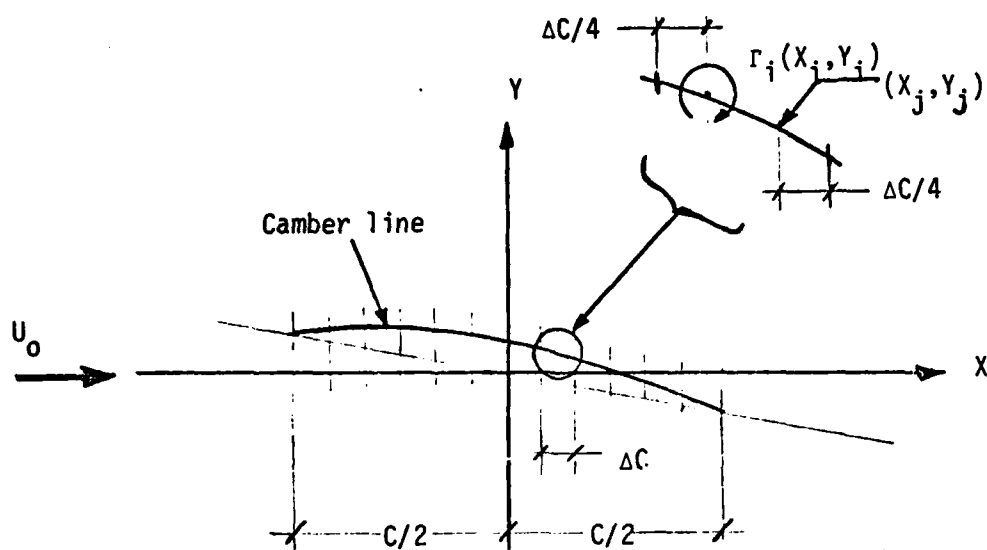


FIGURE 1. Finite Singularity Method

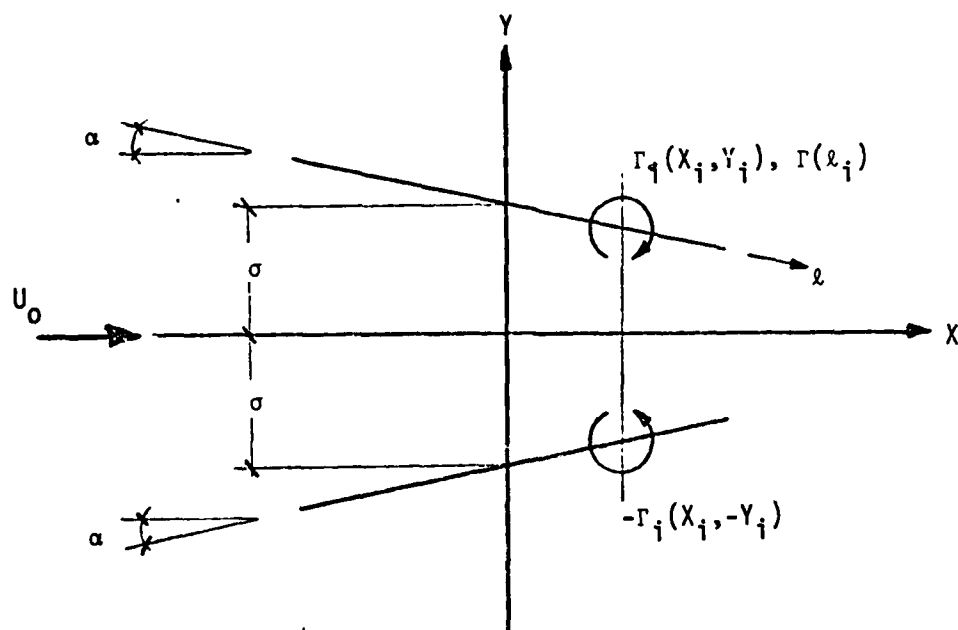


FIGURE 2. Flat Plate in Ground Effect

finite strength is placed at the 25% of each element, points (X_i, Y_i) . The tangential flow boundary condition is satisfied at 75% of each element, points (X_j, Y_j) . The set of algebraic equations to be solved are:

$$U_0 \frac{\partial \gamma}{\partial x} \bigg|_{x_j, y_j} = W(x_j, y_j) = -\frac{1}{2\pi} \sum_{i=1}^N \frac{\Gamma_i (X_i, Y_i) (X_j - X_i)}{(X_j - X_i)^2 + (Y_j - Y_i)^2} \quad j = 1, 2, \dots, N \quad (9)$$

Flat Plate in Ground Effect

As mentioned above, this method is to be applied to a thin symmetric airfoil in ground effect for the purpose of establishing a point of comparison for verification of the finite difference code. In the context of thin airfoil theory a 1% thickness symmetric airfoil appears as a flat plate. Ground effect in the context of the finite singularity method is established by using an image flat plate to satisfy tangential flow on the ground (Fig 2). The tangential flow condition at point (x_j, y_j) in the plate is determined by vortices on both the plate and the image, which leads to the following equation.

$$U_0 \frac{\partial \gamma}{\partial x} \bigg|_{x_j, y_j} = -\frac{1}{2\pi} \sum_{i=1}^N \frac{\Gamma_i (x_j - x_i)}{(x_j - x_i)^2 + (y_j - y_i)^2} + \frac{1}{2\pi} \sum_{i=1}^N \frac{\Gamma_i (x_j - x_i)}{(x_j - x_i)^2 + (y_j + y_i)^2} \quad (10)$$

Substituting the following relations into equation (10)

$$\frac{\partial \gamma}{\partial x} = -\alpha \quad (11)$$

$$X_\kappa = \ell_\kappa \cos \alpha \quad \kappa = i \text{ or } j \quad (12)$$

$$Y_\kappa = a - \ell_\kappa \cos \alpha \quad \kappa = i \text{ or } j \quad (13)$$

gives:

$$-2\pi U_0 \alpha \Big|_{\ell_j} = - \sum_{i=1}^N \frac{\Gamma_i \cdot \cos \alpha}{\ell_j - \ell_i} + \sum_{i=1}^N \frac{\Gamma_i (\ell_j - \ell_i) \cos \alpha}{(\ell_j - \ell_i)^2 \cos^2 \alpha + [2a - (\ell_j + \ell_i) \sin \alpha]^2} \quad (14)$$

Where points ℓ_i, ℓ_j are calculated for N equal elements as:

$$\ell_i = (-0.5 + \frac{i-1}{N} + \frac{0.25}{N}) \cdot C \quad i = 1, \dots, N \quad (15)$$

$$\ell_j = (-0.5 + \frac{j-1}{N} + \frac{0.25}{N}) \cdot C \quad j = 1, \dots, N \quad (16)$$

Equation (14) is written in a matrix form

$$-2\pi U_0 \alpha = \cos \alpha \cdot [A] \{\Gamma_i\} \quad (17)$$

The vortex strengths are obtained by inverting matrix A.

$$\{\Gamma_i\} = \frac{-2\pi U_0 \alpha}{\cos \alpha} [A^{-1}] \quad (18)$$

Integrating equations (7) and (8) numerically provides the lift and moment coefficients

$$C_\ell = \frac{2 \cdot \cos \alpha}{U_0 \cdot C} \sum_{i=1}^N \Gamma_i \quad (19)$$

$$C_{m_{c/4}} = \frac{2 \cos \alpha}{U_0 C^2} \sum_{i=1}^N (\frac{C}{4} - \ell_i) \cdot \Gamma_i \quad (20)$$

Equations (18), (19), and (20) are solved numerically for 20 equal length elements.

Results

Tabulated and graphic representation (Tables 1 and 2, Figs 3÷6) of lift and quarter chord moment coefficients as function of ground distance

and angle of attack, are shown. The results indicate an increase in lift coefficient and pitch down quarter chord moment coefficient, for a given angle of attack as the airfoil approaches the ground. The increase in lift and pitch down quarter chord moment coefficients start to be significant when the ground distance equals the chord length and less. The obtained results will be compared against those obtained by the finite difference method in Chapter V.

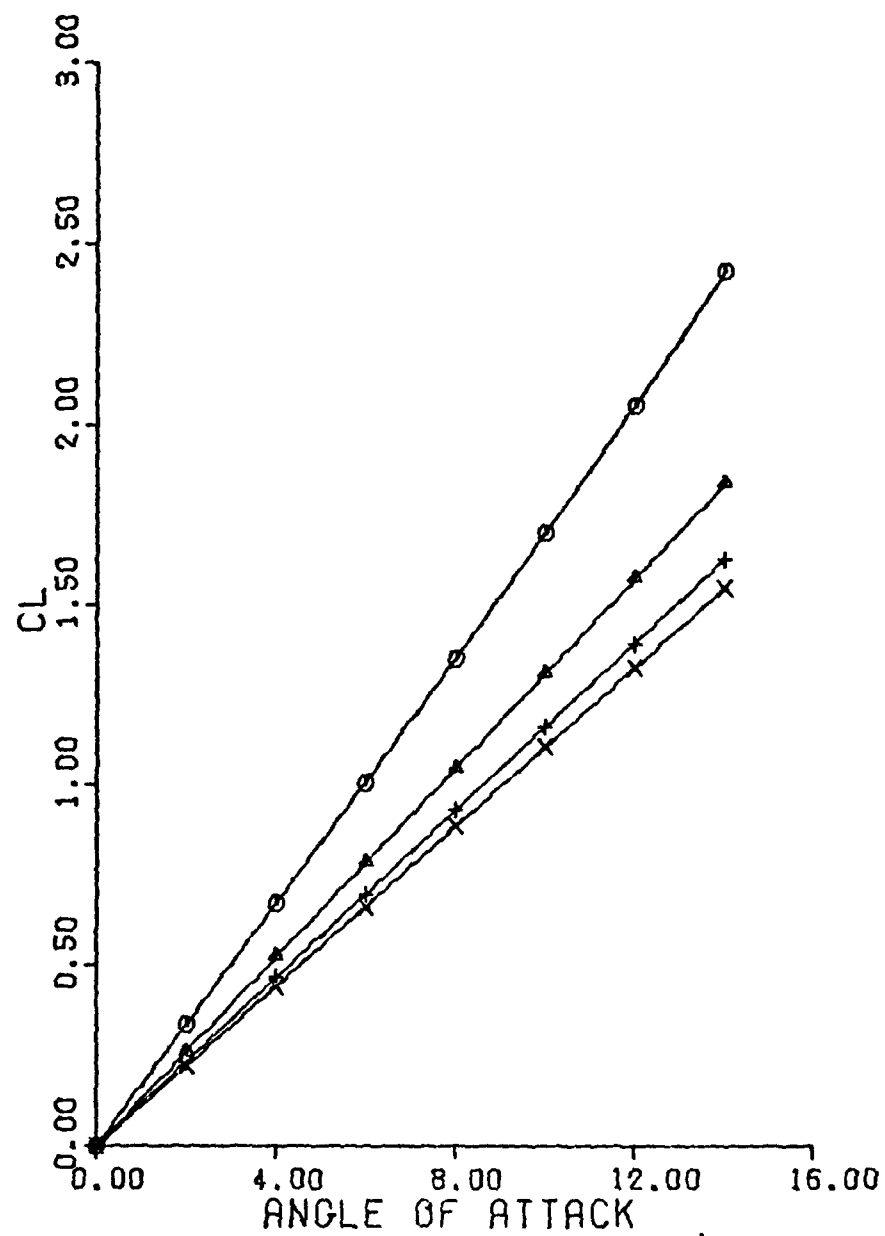


FIGURE 3. Lift Coefficient vs. Angle of Attack
Ground distance as a Parameter

θ - 0.25C

Δ - 0.50C

+ - 1.00C

X - Free Stream

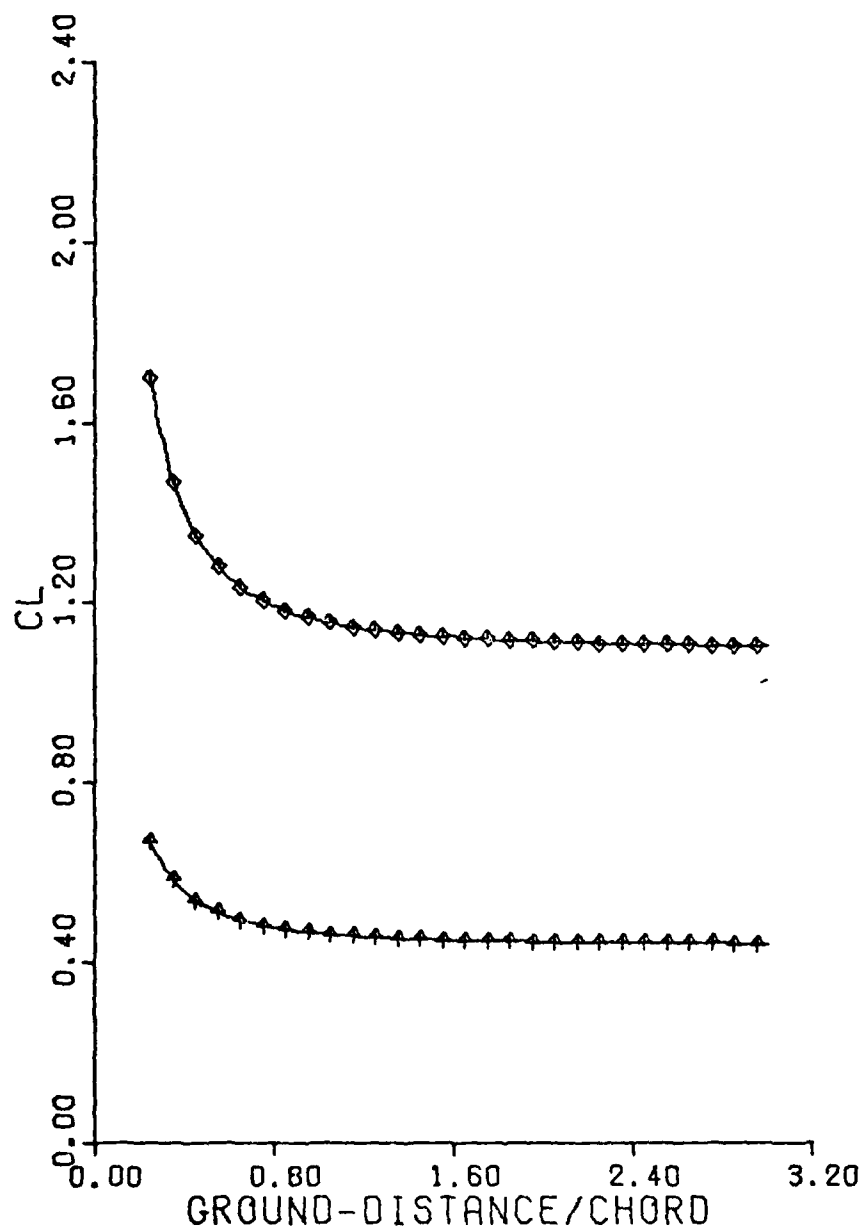


FIGURE 4. Lift Coefficient vs. Ground Distance.
Angle of Attack as a Parameter.

$\diamond - 10^\circ$, $\triangle - 4^\circ$

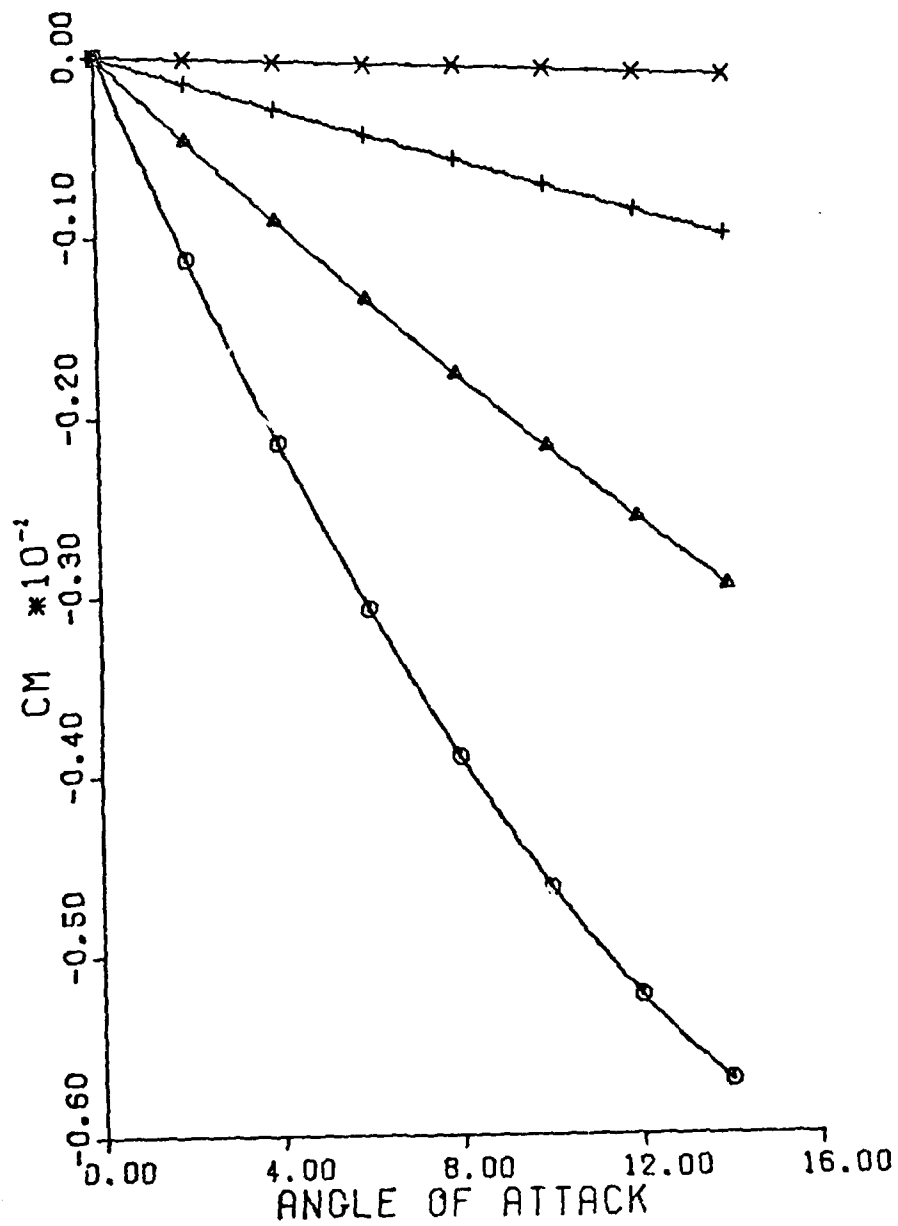


FIGURE 5. Quarter-Chord Moment Coefficient vs. Angle of Attack
Ground Distance as a parameter.

\circ - 0.25c

Δ - 0.50c

$+$ - 1.00c

\times - Free stream

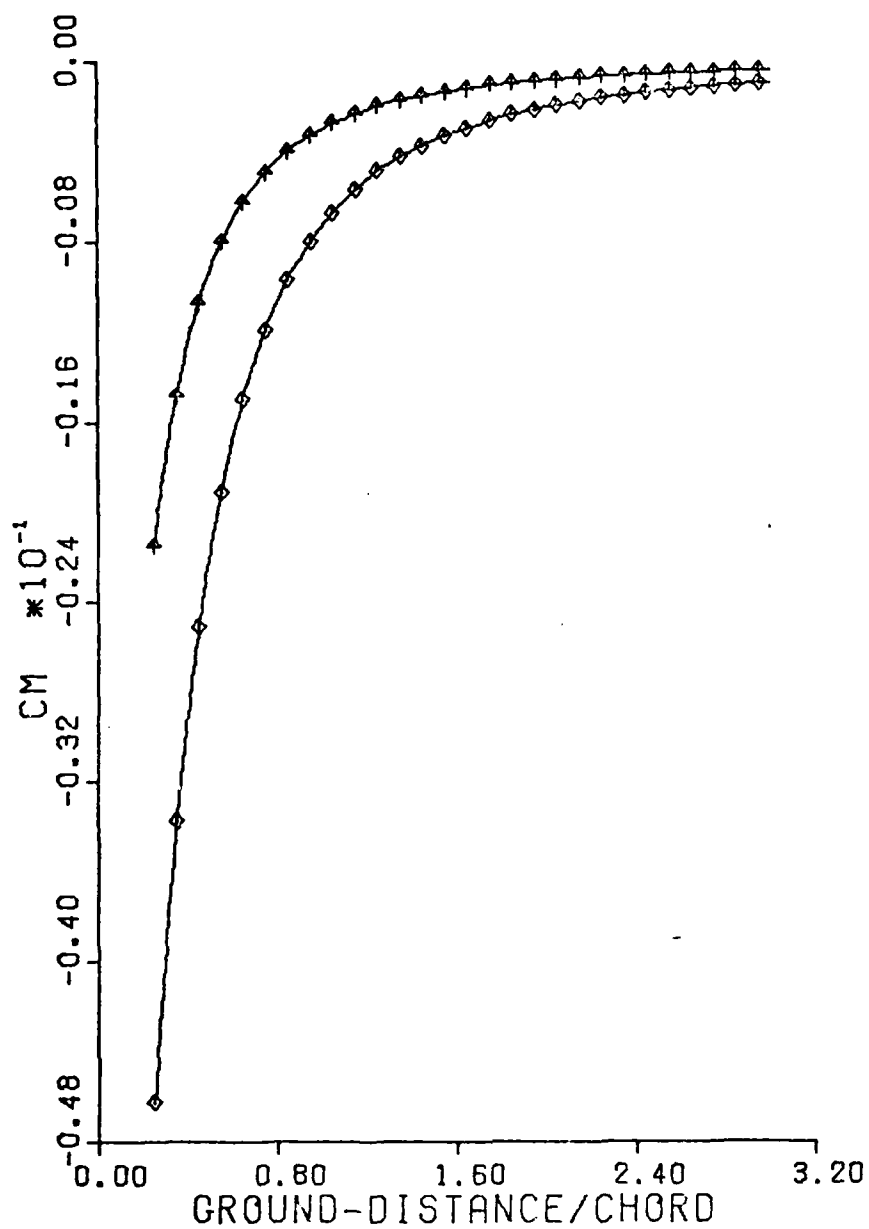


FIGURE 6. Quarter-Chord Moment Coefficient vs. Ground Distance.
Angle of Attack as a Parameter
 $\diamond - 10^\circ$, $\triangle - 40^\circ$

TABLE 1. Lift Coefficient as Function of Angle of Attack
and Ground Distance - Finite Singularity Method

α	GROUND DISTANCE			
	INFINITY	1.00	0.50	0.25
0.0	0.00	0.00	0.00	0.00
1.0	.11	.12	.12	.17
2.0	.22	.23	.25	.33
3.0	.33	.35	.39	.50
4.0	.44	.46	.52	.67
5.0	.55	.58	.65	.84
6.0	.66	.70	.78	1.01
7.0	.77	.81	.92	1.18
8.0	.88	.93	1.05	1.35
9.0	.99	1.04	1.18	1.52
10.0	1.10	1.16	1.31	1.70

TABLE 2. Quarter Chord Moment Coefficient as Function
of Angle of Attack and Ground Distance -
Finite Singularity Method

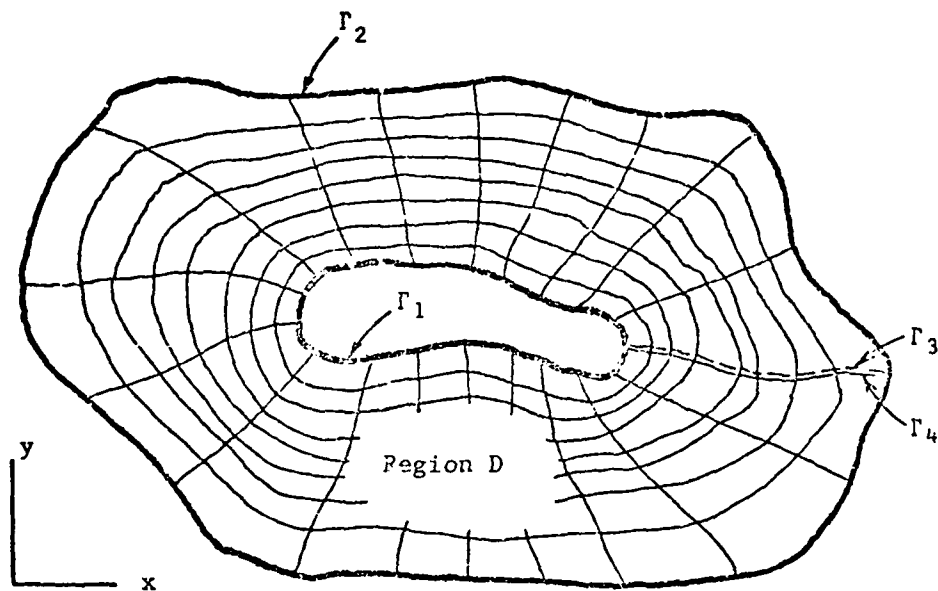
α	GROUND DISTANCE			
	INFINITY	1.00	0.50	0.25
0.0	0.00000	0.00000	0.00000	0.00000
1.0	-.00000	-.00076	-.00237	-.00578
2.0	-.00000	-.00151	-.00470	-.01129
3.0	-.00000	-.00226	-.00698	-.01654
4.0	-.00000	-.00300	-.00922	-.02154
5.0	-.00000	-.00374	-.01142	-.02629
6.0	-.00000	-.00446	-.01357	-.03079
7.0	-.00000	-.00519	-.01563	-.03504
8.0	-.00000	-.00590	-.01777	-.03905
9.0	-.00000	-.00662	-.01982	-.04279
10.0	-.00000	-.00732	-.02183	-.04627

III. COORDINATE TRANSFORMATION

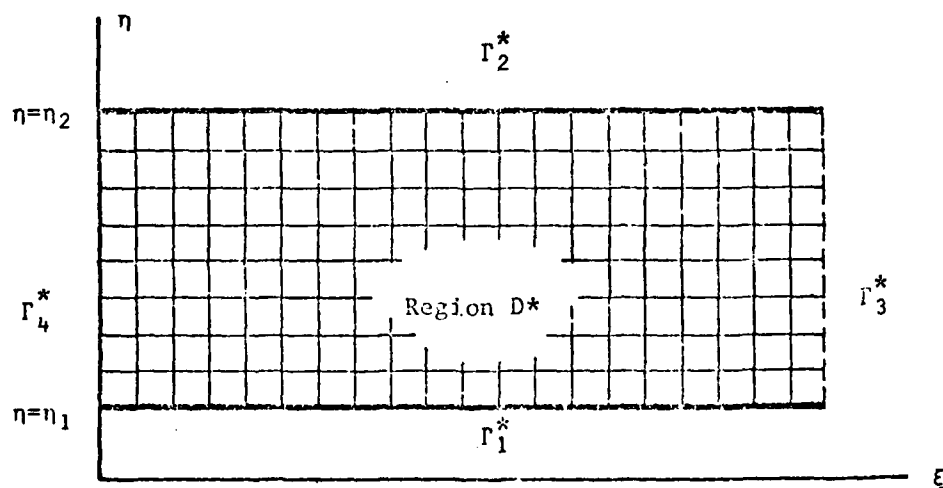
Coordinate transformation (or generation of boundary fitted coordinate system) is a general method that can be used for multiple bodies with arbitrary boundaries. The method can be used for solution of any type of partial differential equations. The mathematical background and development are described in detail in Ref 4. In this work the method is used to solve the stream function equation for various boundaries and boundary conditions. In this chapter a very brief discussion of the method is introduced.

Mathematical Development

For purposes of discussion in this work the region of interest is two dimensional and doubly connected. The solution of all the partial differential equations is done in the transformed plane which is rectangular in shape and has a square mesh. Figure 7 illustrates an arbitrary two dimensional doubly connected region with arbitrary inner and outer boundaries that is transferred into a rectangular region. The inner contour maps into the η_1 line and the outer contour maps into the η_2 line. The contours connecting the inner and outer boundaries map into ξ_{min} and ξ_{max} . Since they coincide in the physical plane, they constitute re-entrant boundaries in the transformed plane. This type of mapping is used for all transformations in this work. The coordinates of each grid point in the physical plane are generated as solutions of Poisson equations in the physical plane, with Dirichlet boundary conditions on all boundaries. Control functions P and Q appear as inhomogeneous terms in the Poisson equations, that are:



Physical Plane



Transformed Plane

Figure 7. Field Transformation - Single Body
(from Ref 4, p. 170)

$$\xi_{xx} + \xi_{yy} = P(\xi, \eta) \quad (21)$$

$$\eta_{xx} + \eta_{yy} = Q(\xi, \eta) \quad (22)$$

This system in the transformed form becomes:

$$\alpha X_{\xi\xi} - 2\beta X_{\xi\eta} + \gamma X_{\eta\eta} + J^2 (PX_{\xi} + QX_{\eta}) = 0 \quad (23)$$

$$\alpha Y_{\xi\xi} - 2\beta Y_{\xi\eta} + \gamma Y_{\eta\eta} + J^2 (PY_{\xi} + QY_{\eta}) = 0 \quad (24)$$

Where α , β , γ , J are functions of first order partial derivatives of the physical coordinates (X, Y) with respect to transformed coordinates (ξ, η) . This type of mapping physical boundaries into the transformed plane is arbitrary and not limited to the mapping described above.

Coordinate System Control

Spacing of coordinate lines on the boundaries is accomplished easily as boundaries points are given as input data. Also, the coordinate lines that map into ξ_{\max} and ξ_{\min} in the transformed plane are easily controlled by input data. However, a spacing of coordinate lines within the field is controlled by varying the elliptic generating system (changing P and Q).

In the control system used, P is zero and Q is a sum of exponential terms with various coefficients, to attract constant η lines to the body. The coefficients have been calculated for a flat plate to ensure sufficient constant η lines in the boundary layer. Those P and Q functions were programmed for airfoil calculations in viscous flow, and are less important for potential flow calculation considered here. Consequently, slight attraction of constant η lines to the airfoil is used for free stream airfoil calculations and Q is set to zero in all other cases.

Difference Equations

The governing differential equations are approximated by second order central difference expressions. The number of constant ξ lines is designated IMAX and the number of constant η lines by JMAX, the computational field is $(JMAX-2) \cdot (IMAX-1)$. In the computer program (Appendix A) that is used the standard field size is 71×44 . The boundary mapping described previously is such as $J=1$ and $J=JMAX$ correspond to the inner and outer boundaries. The inner contour (the body) is given by 71 pairs of (x,y) data points, the outer boundary is either given in the same manner or is calculated in the program. An initial guess is generated in the program. Because the difference equations are nonlinear, the initial guess must be within a certain neighborhood of the solution if the iterative solution is to converge. Boundary input data and initial guess type for the various regions are discussed in Chapters V and VI. Difference equations are solved by a SOR (Successive Over Relaxation) iterative scheme. The acceleration parameter of the SOR scheme was usually set equal to one, since the objective of this study is not optimization of transformation computer time.

Transformation Properties

The transformation procedure described above holds several benefits and properties.

1. Numerical solution of partial differential equations may be done in the transformed plane and on a fixed rectangular grid with square mesh. Even though the partial differential equation is complicated by the transformation, the numerical scheme does not have to compensate for grid changes.

2. No interpolation is required to locate boundary points regardless of the physical field. This property is of particular importance for boundaries with strong curvature such as an airfoil leading edge.

3. Even time dependent boundaries transform to a fixed rectangular grid with square mesh, but the transformation equations (23 and (24) must be re-solved at each time step, which changes α, β, γ, J as well as the coordinate system in the physical plane at each time step.

4. The coordinate system generated by equations (23) and (24) is not necessarily orthogonal but it is a general solution for arbitrary spacing and capability of concentration of coordinate lines. This generality outweighs the lack of orthogonality.

5. The partial differential equation type (elliptic, parabolic, hyperbolic) remains invariant under the transformation.

Applications

Generation of specific boundary fitted coordinated systems for the various boundaries chosen to solve the flow field for an airfoil in both free stream and ground effect are described in Chapter V. The coordinate system for the hovercraft model is described in Chapter VI.

As a simple verification of the computer program, two boundary fitted coordinate systems were generated for the region between two concentric circles of one and ten units diameter. Equally spaced concentric circles were used as an initial guess in each case. The first coordinate system was computed without attraction of coordinate lines ($P = Q = 0$ in equation (23) and (24)), where the expected and derived coordinate system consisted of concentric circles (Figs 8 and 9). The same region

is solved the second time with slight attraction to the inner circle leading edge (point $(-0.5,0)$), the attraction can easily be noticed in Fig 10.

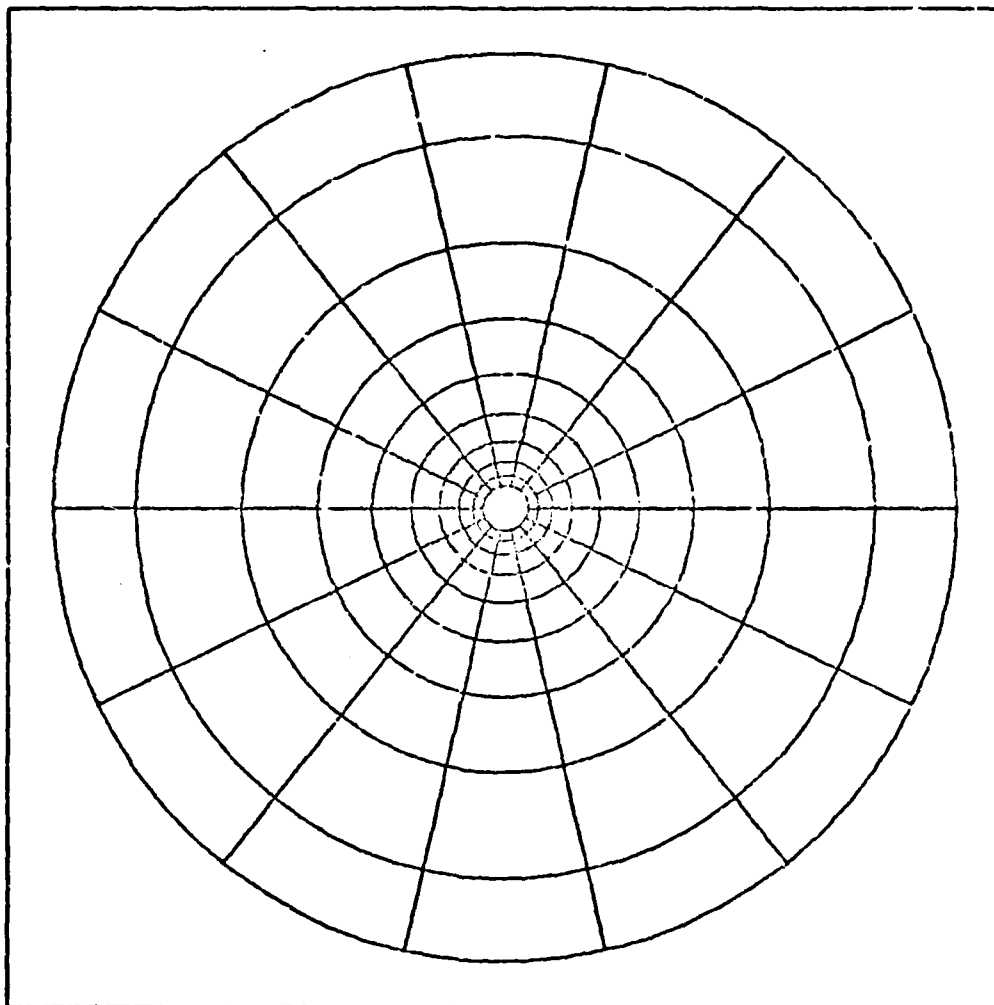


FIGURE 8. Body-Fitted Coordinate System for a Cylinder in a Circular Outer Boundary (Entire region). Each fifth ξ and η line are shown.

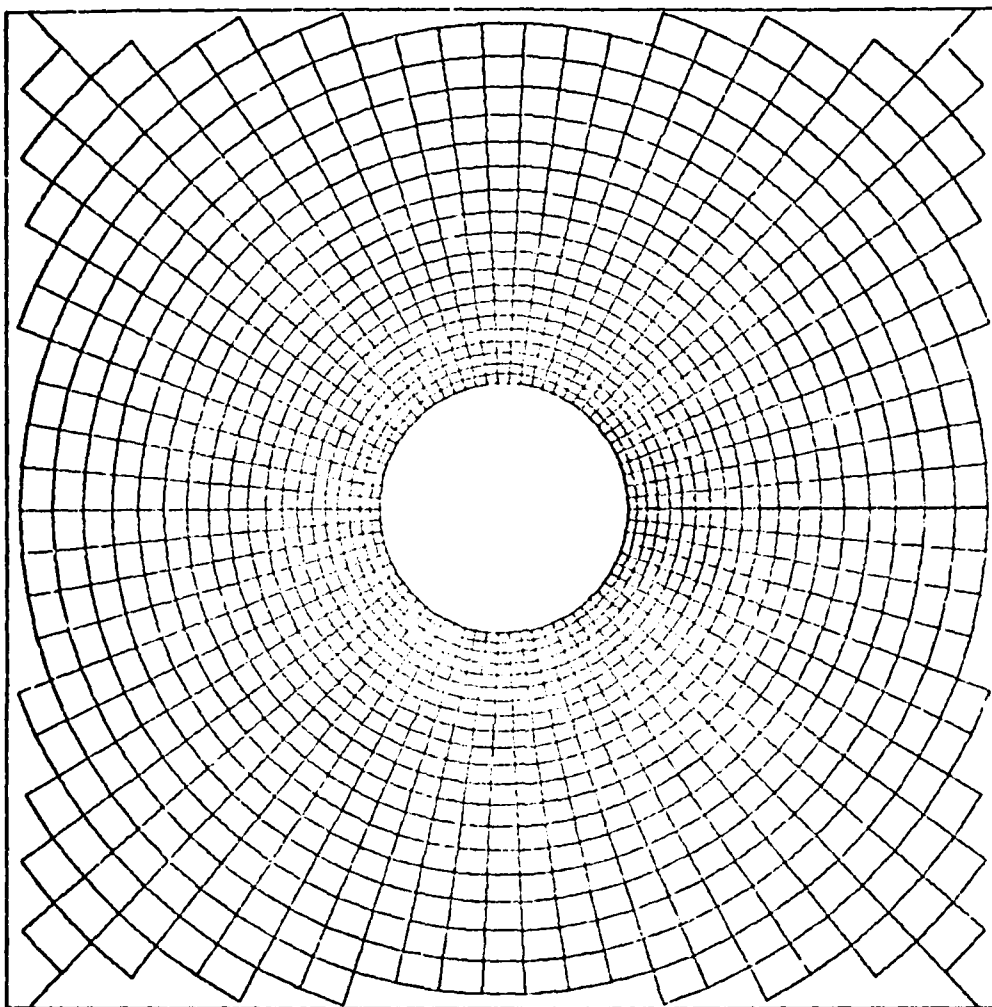


FIGURE 9. Body Fitted Coordinate System for a Cylinder in a Circular Outer Boundary. No Attraction of Coordinates ($P = Q = 0$)

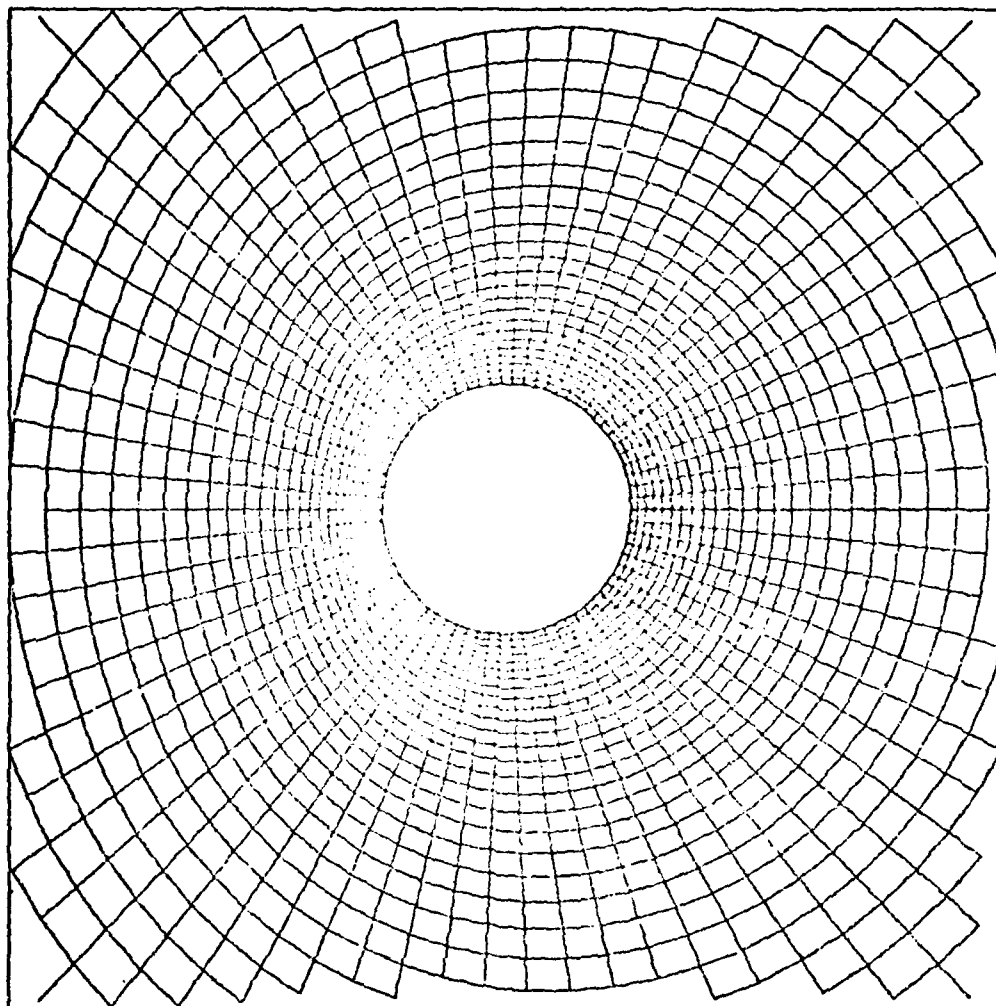


FIGURE 10. Body-Fitted Coordinate System for a Cylinder in a Circular Outer Boundary. Attraction of Constant η Coordinates.

IV. STREAM FUNCTION SOLUTION

Any set of partial differential equations may be solved on the boundary fitted coordinate system by transforming the equations and associated boundary conditions and solving numerically in the transformed plane. In particular, the method is applied here to solve the stream function equation.

Differential Equation and Aerodynamic Coefficients

Two dimensional potential flow about an airfoil is described by Laplace equation for the stream function.

$$\psi_{xx} + \psi_{yy} = 0 \quad (25)$$

The simplest boundary conditions are Dirichlet type where values are specified on the boundaries

$$\psi(x,y) = \psi_1(x,y) \text{ on the body} \quad (26)$$

$$\psi(x,y) = \psi_2(x,y) \text{ on the outer boundary} \quad (27)$$

Equation (25) and boundary conditions (26) and (27) after transformed are:

$$\alpha\psi_{\xi\xi} + 2\beta\psi_{\xi\eta} + \gamma\psi_{\eta\eta} + \sigma\psi_{\eta} + \tau\psi_{\xi} = 0 \quad (28)$$

$$\psi(\xi, \eta_{\min}) = \psi_1(\xi, \eta_{\min}) \quad (29)$$

$$\psi(\xi, \eta_{\max}) = \psi_2(\xi, \eta_{\max}) \quad (30)$$

For this case of irrotational flow the Bernoulli equation holds for the entire field, and, for stream function that is nondimensionalized relative to the airfoil chord and free stream velocity, we find on the body surface

$$C_p = 1 - \frac{\gamma}{J^2} \psi_n^2 \quad (31)$$

In our case the free stream is in positive x direction and therefore the integration of C_p to obtain lift and quarter chord moment coefficients leads to:

$$C_l = - \int_{\xi_{\min}}^{\xi_{\max}} C_p X_{\xi} d\xi \quad (32)$$

$$C_{m_{c/4}} = \int_{\xi_{\min}}^{\xi_{\max}} C_l \left(\frac{X}{C} + \frac{C}{4} \right) d\xi \quad (33)$$

$\alpha, \beta, \gamma, \sigma, \tau, J$ in the above equations are functions of partial derivatives of the physical coordinates (x, y) with respect to transformed coordinates (ξ, η) (Ref 4, Appendix A). It should also be noted that using the Bernoulli equation to calculate pressure distribution is a correct approach for an irrotational flow field. Solution of a flow field for a hovercraft is different in nature and the differences are discussed in Chapter VI.

Difference Equation

Equation (28) is approximated by second-order difference expressions on the transformed grid. For the chosen field size, 71 x 44, Dirichlet boundary conditions are specified by

$$\psi(I,J) = \psi_1(I,1) \text{ on the body} \quad (34)$$

$$\psi(I,J) = \psi_2(I,44) \text{ on the outer boundary} \quad (35)$$

An explicit scheme is used to solve the stream function field. The difference equation corresponding to equation (28) is

$$\begin{aligned} x_{i,j}^{n+1} = & [\tilde{\alpha}_{i,j}(\psi_{i-1,j} + \psi_{i+1,j}) - \tilde{\beta}_{i,j}(-\psi_{i-1,j+1} + \psi_{i+1,j+1} + \psi_{i-1,j-1} - \psi_{i+1,j-1}) \\ & + \tilde{\gamma}_{i,j}(\psi_{i,j-1} + \psi_{i,j+1}) + \tilde{\sigma}_{i,j}(-\psi_{i,j-1} + \psi_{i,j+1}) + \tilde{\tau}_{i,j}(-\psi_{i-1,j} + \psi_{i+1,j})]^n \end{aligned} \quad (36)$$

$$T = 2(\alpha_{i,j} + \gamma_{i,j}) \quad (37)$$

$$(\tilde{\alpha}_{i,j}; \tilde{\beta}_{i,j}; \tilde{\gamma}_{i,j}; \tilde{\sigma}_{i,j}; \tilde{\tau}_{i,j}) = (\alpha_{i,j}; \beta_{i,j}/2; \gamma_{i,j}; \sigma_{i,j}/2; \tau_{i,j}/2)/T \quad (38)$$

Where superscript n refers to the most recent stream function values.

Starting from an initial guess for stream function values over the computational field, iteration with equation (36) converges to the solution.

The pressure coefficient equation (31) is evaluated on the body and, as the body maps to J=1 line, ψ_η is approximated by second order one-sided difference expression. Integrating the pressure coefficient into lift and quarter chord moment coefficients (Equations (32) and (33)) is accomplished by using Simpson's one-third numerical integration algorithm. For computer programs see Appendix A.

Applications

Stream function solutions for an airfoil in free stream and ground effect are given in Chapter V and stream function contour plot are shown too. Modifications of the above equations to include multi-valued points

(branch cut) and vorticity to accommodate for the hovercraft peripheral jet flow field solution are introduced in Chapter VI.

To check the equations and computer programs that are used, the pressure coefficient variation for a cylinder in uniform flow is computed using the coordinate system generated as described in the previous chapter. As shown in Fig 11, good correlation is achieved between the analytical and the finite difference solutions. Stream function contour lines for this case are shown in Fig 12.

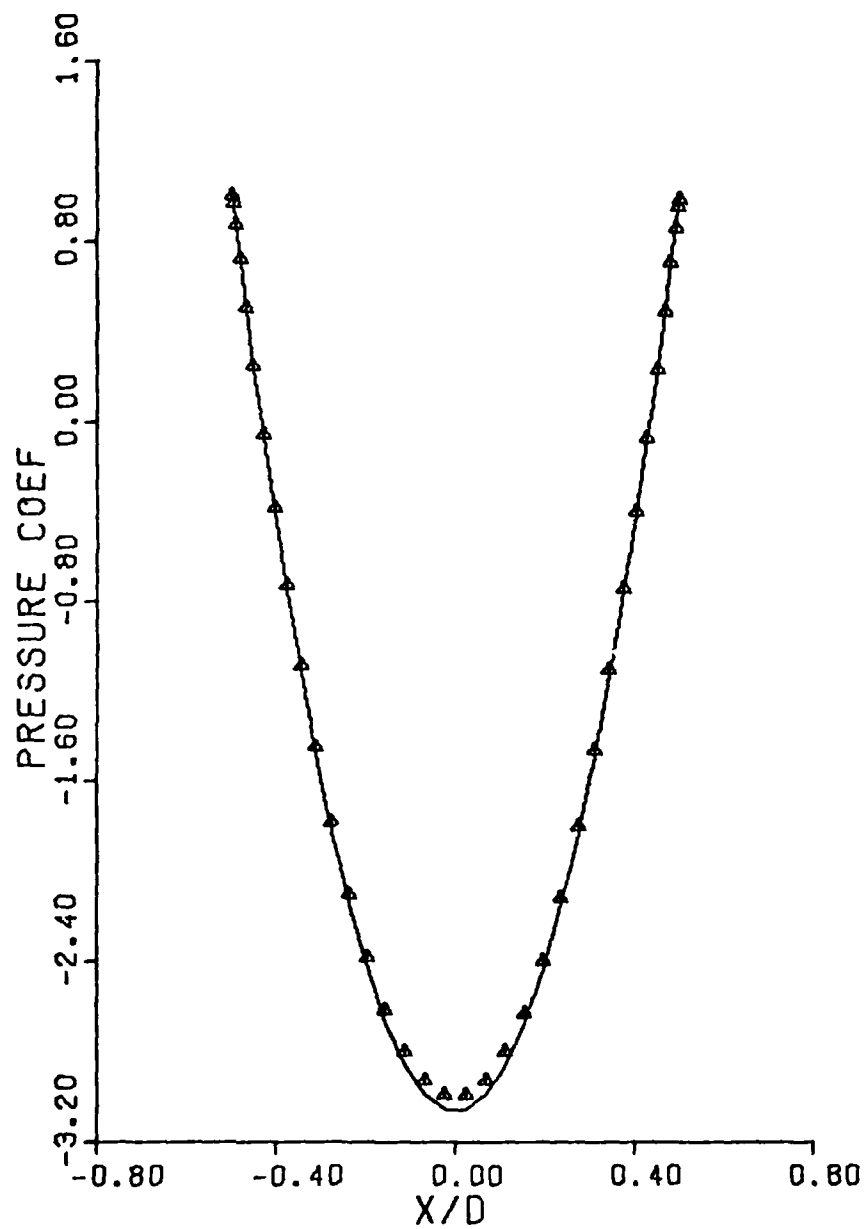


FIGURE 11. Pressure Coefficient on a Cylinder vs. Nondimensionalized Diameter in Free Stream Direction

— Analytical
△ Finite Difference

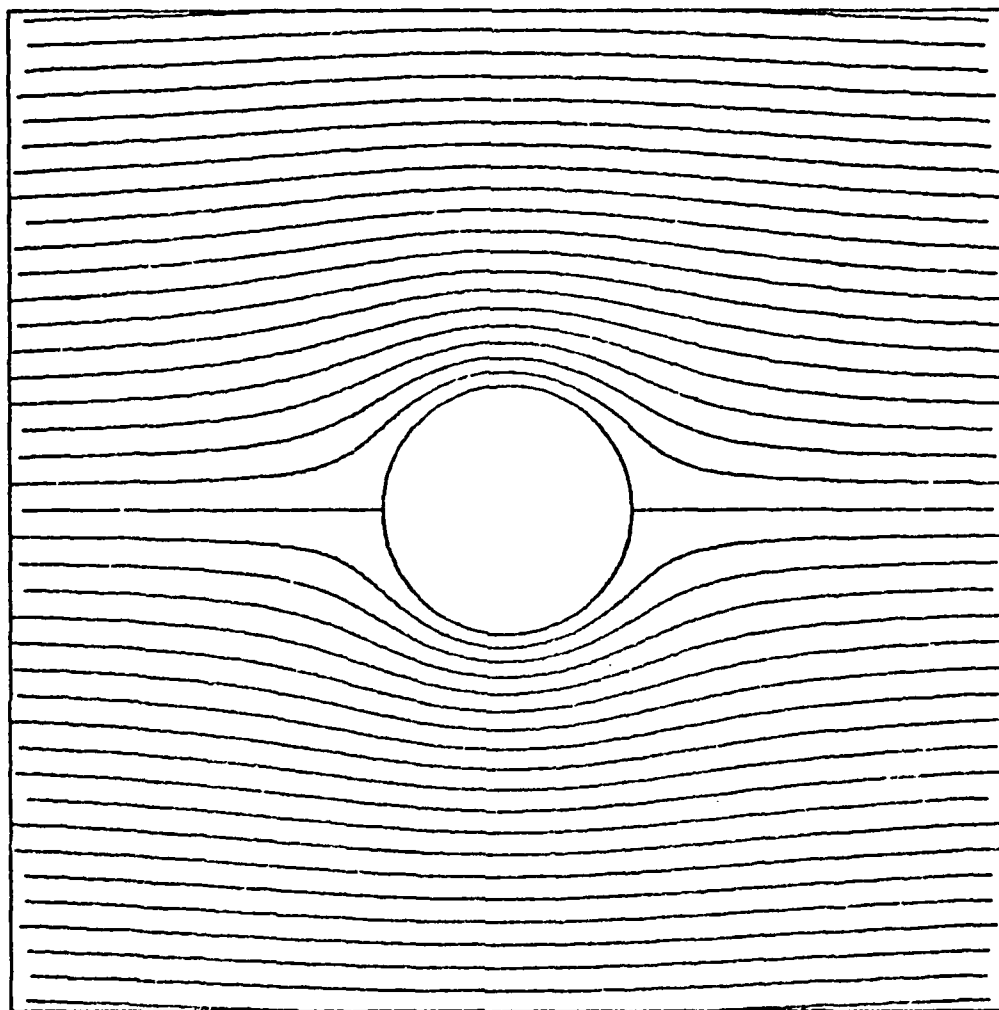


FIGURE 12. Stream Function Contour Plot for Cylinder in Free Stream

V. AIRFOIL STREAM FUNCTION SOLUTION

This chapter describes the numerical solution for airfoil in free stream and ground effect. Included are details of the generation of boundary fitted coordinate system, the determination of a stream function solution with the Kutta condition satisfied at the leading edge, and the derivation of lift and quarter-chord moment coefficients.

Airfoil Type

The procedure used is applicable to any arbitrary airfoil for which the flow remains attached. For simplicity and to permit a comparison with results derived by finite singularity method (Chapter II), a thin airfoil was chosen. The finite singularity method was solved for a flat plate, therefore for stream function solution a symmetric 1% thickness ratio airfoil is used. The determination of the grid points distribution around the airfoil without interpolation between data points can be achieved by using a NACA four-digit airfoil that can be described by an equation (Ref 5). Consequently, the chosen airfoil can be designated as NACA 0001.

Kutta Condition

Ordinarily, the Kutta condition at the trailing edge of an airfoil can be stated in terms of either velocities or pressure differences. The most convenient manner of stating Kutta condition in our case is in terms of the stream function. Specifically, the body stream function must detach from the airfoil at the trailing edge with the local camber line slope. The procedure for stream function solution with Dirichlet boundary conditions requires that a value for the body stream function be specified and an arbitrary value will not necessarily satisfy the Kutta condition.

Thus, the computation of a stream function solution which does satisfy the Kutta condition requires an iteration and interpolation upon the value chosen for the body streamline. Three points are chosen from the field solution; one is the trailing edge, and the other two are slightly behind the trailing edge and located on opposite sides of the extension of trailing edge camber line. The physical coordinates and the stream function values are known in these points that are marked as 1, 2 and 3 (Fig 13).

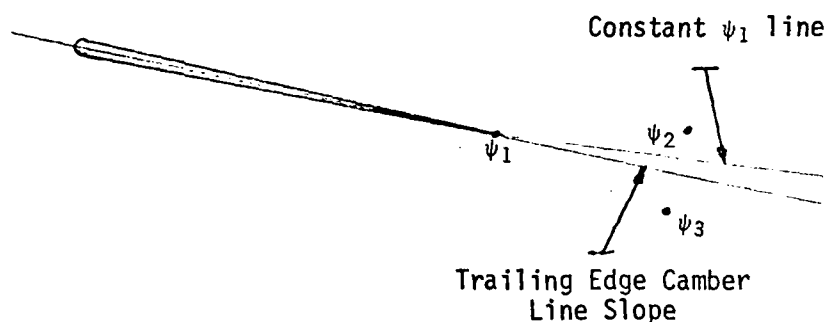


Figure 13. Kutta Condition Check Scheme

Equation of the plane passing through the three points is

$$\begin{vmatrix} X & Y & \psi & 1 \\ X_1 & Y_1 & \psi_1 & 1 \\ X_2 & Y_2 & \psi_2 & 1 \\ X_3 & Y_3 & \psi_3 & 1 \end{vmatrix} = 0 \quad (39)$$

Substituting $\psi = \psi_1$ in equation (39) the plane equation reduces to a straight line equation passing through the trailing edge with the

stream function value ψ_1 constant along the straight line. The slope of the straight line is given by

$$\left(\frac{dY}{dX}\right)_{T.E.} = \frac{Y-Y_1}{X-X_1} = \frac{(Y_2-Y_1)(\psi_3-\psi_1)-(Y_3-Y_1)(\psi_2-\psi_1)}{(X_2-X_1)(\psi_3-\psi_1)-(X_3-X_1)(\psi_2-\psi_1)} \quad (40)$$

The Kutta condition is said to be satisfied whenever the slope derived by equation (40) is in the proximity of the trailing edge camber line slope within specified allowable error.

Airfoil in Free Stream

The airfoil is the inner boundary for generation of body fitted coordinate system. The point collection describing the airfoil contour is calculated by the equation for NACA 0001 airfoil (Table 3). The origin for the region is at the mid-chord which is nondimensionalized to unit length. In order to use the same airfoil point distribution for free stream and ground effect cases, the airfoil is rotated clockwise by the angle of attack. The boundary fitted coordinate system has to be re-generated for each angle of attack. The "infinity" outer boundary is a circle of ten chord length radius, which is described by equally spaced points on the circumference. The airfoil points are numbered from the trailing edge clockwise and the points on the outer boundary are numbered for point (10,0) also clockwise. The outer boundary is generated by a program subroutine. The initial guess is a series of elliptical n lines with an increasing interval in axial direction. A typical body fitted coordinate system is shown in Fig 14 and an enlargement and more detailed picture of the airfoil neighborhood is given in Fig 15.

The stream function is computed in the transformed plane from the transformed Laplace equation. Stream function values for a uniform flow

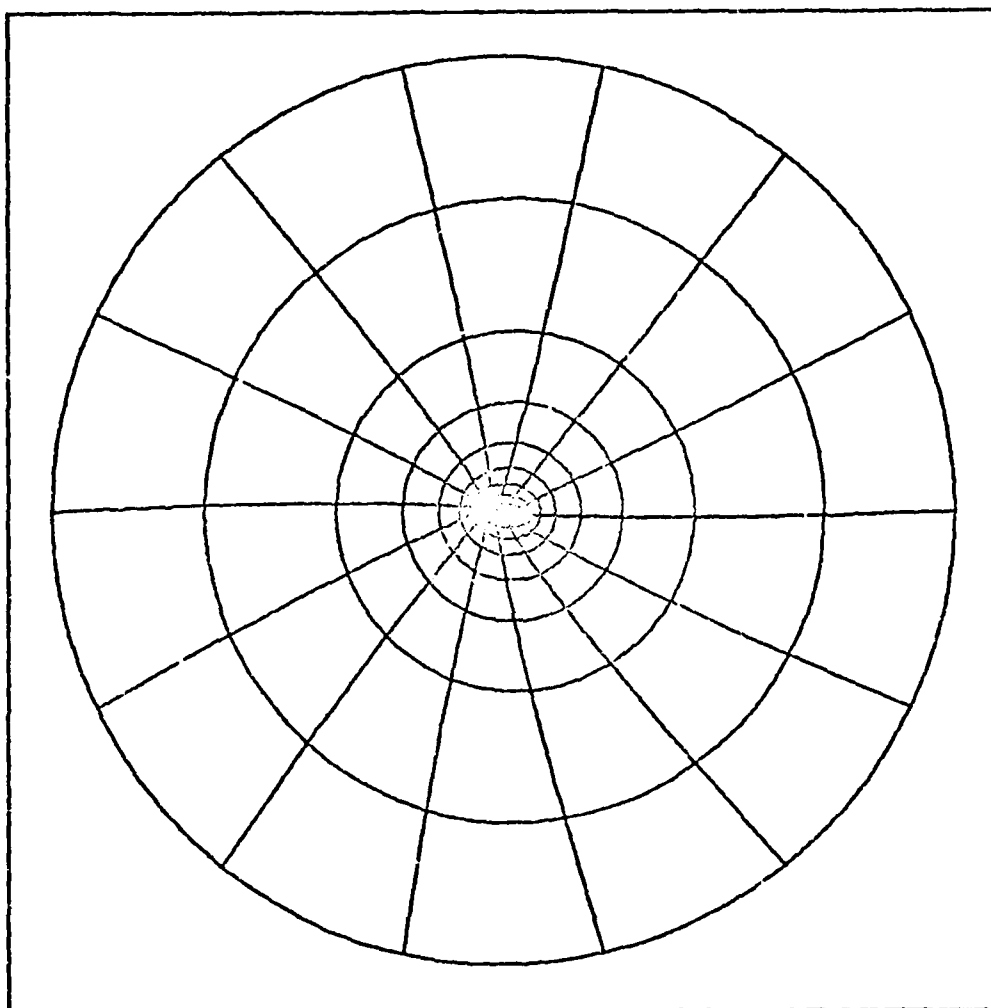


FIGURE 14. Body Fitted Coordinate System for Airfoil in Free Stream. Each fifth ξ and η lines are shown.

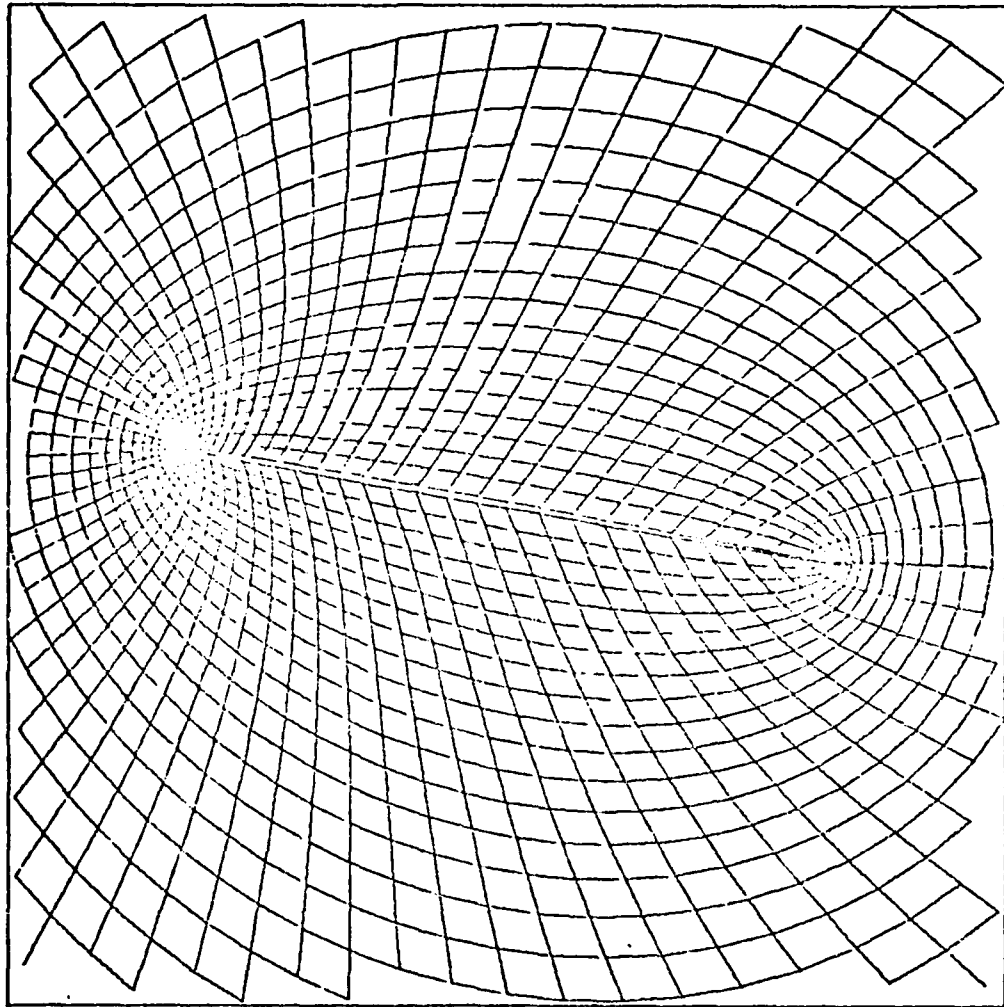


FIGURE 15. Body Fitted Coordinate System for Airfoil
in Free Stream, Partial Region

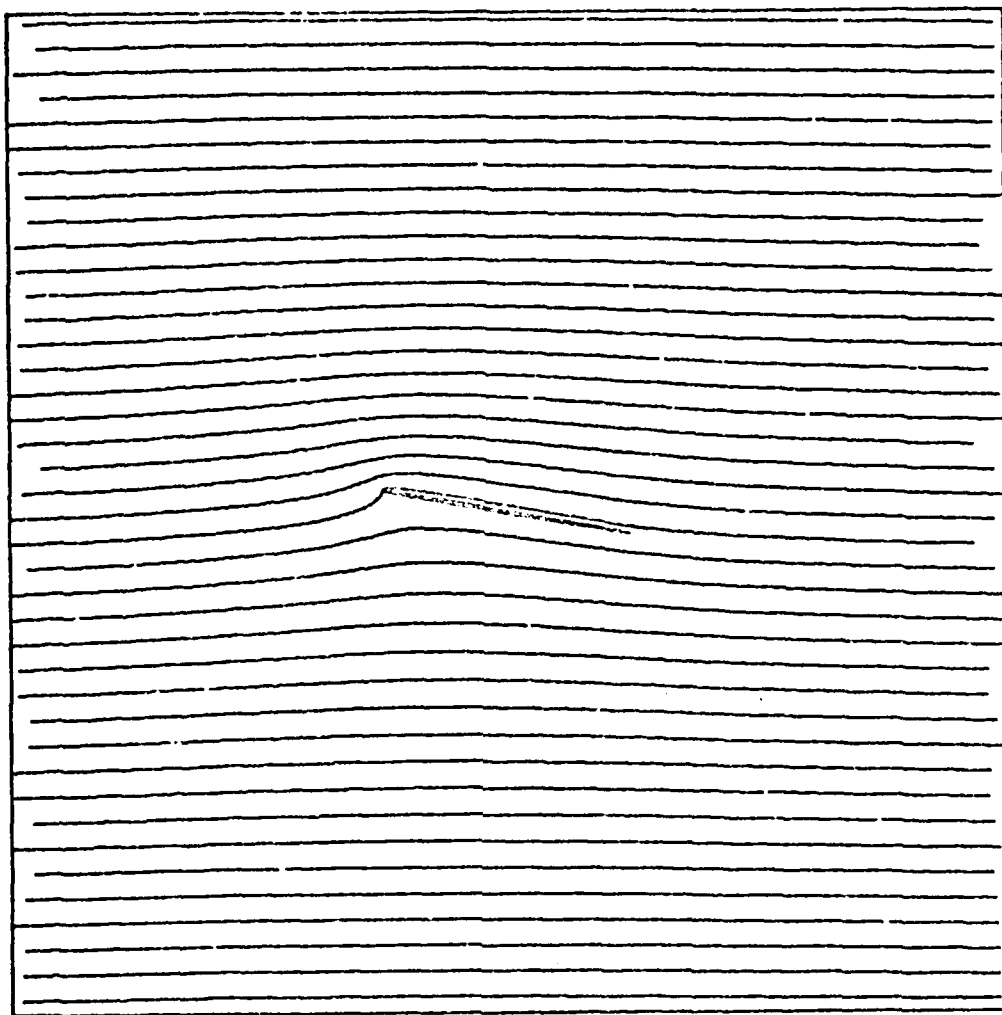


FIGURE 16. Stream Function Contour Plot for Airfoil in 10° Angle of Attack in Free Stream.

TABLE 3. Numerical Data for an Airfoil in
10° Angle of Attack

POINT	X	Y	POINT	X	Y
1	.4924	-.0868	37	-.4923	.0869
2	.4430	-.0788	38	-.4921	.0870
3	.3937	-.0706	39	-.4917	.0871
4	.3444	-.0625	40	-.4912	.0871
5	.2951	-.0542	41	-.4906	.0871
6	.2457	-.0460	42	-.4899	.0871
7	.1964	-.0377	43	-.4895	.0868
8	.1471	-.0294	44	-.4790	.0861
9	.0978	-.0211	45	-.4704	.0850
10	.0485	-.0127	46	-.4597	.0836
11	-.0008	-.0043	47	-.4469	.0817
12	-.0451	.0033	48	-.4320	.0794
13	-.0919	.0113	49	-.4150	.0768
14	-.1360	.0190	50	-.3958	.0737
15	-.1776	.0262	51	-.3720	.0698
16	-.2167	.0331	52	-.3457	.0655
17	-.2531	.0396	53	-.3168	.0606
18	-.2871	.0457	54	-.2854	.0552
19	-.3184	.0514	55	-.2514	.0493
20	-.3472	.0567	56	-.2149	.0430
21	-.3735	.0616	57	-.1759	.0361
22	-.3972	.0661	58	-.1343	.0287
23	-.4162	.0698	59	-.0902	.0208
24	-.4331	.0731	60	-.0435	.0124
25	-.4479	.0761	61	.0008	.0043
26	-.4606	.0787	62	.0500	-.0016
27	-.4711	.0810	63	.0991	-.0136
28	-.4795	.0829	64	.1484	-.0227
29	-.4859	.0845	65	.1975	-.0317
30	-.4901	.0857	66	.2467	-.0408
31	-.4938	.0869	67	.2950	-.0499
32	-.4964	.0879	68	.3430	-.0591
33	-.4981	.0884	69	.3941	-.0683
34	-.4992	.0885	70	.4433	-.0775
35	-.4996	.0887	71	.4924	-.0868
36	-.4994	.0888			

at zero angle of attack and a guess for the body stream function value are used as boundary conditions. The initial guess is also the stream function field for a uniform flow at zero angle of attack. A second guess for the body stream function value is used and the stream function fields are solved for those two guesses. The extent to which the solution corresponding to each body stream function value satisfies the Kutta condition is noted for each case. Then, assuming that the discrepancy in Kutta condition is a linear function of body stream function value, a new value for body stream function value is determined. Thus, an iterative procedure with linearly interpolated values for body stream function is started. Iterations are said to converge to the final result when the stream function slope at the trailing edge equals the airfoil camber line slope at this point within allowable error. Contour stream function plots (Fig 16) illustrates satisfaction of Kutta condition.

Different grid point distributions have been tried for airfoil representation. The very first distribution with equally spaced chordwise intervals did not follow the curvature of the leading edge and produced a sharp leading edge. This case was not used. The leading edge was next smoothed by distributing 11 out of a total of 71 points in the 0.05 chord length from the leading edge. The remaining parts were equally spaced beyond this point. Thus the equation for X location of grid points for an airfoil in zero angle of attack is:

$$\begin{aligned} X^* &= 0.5 - \frac{0.95}{30} (k-1) & k &= 1, \dots, 30 \\ &= 0.45 - \frac{0.05}{6} (k-30) & k &= 31, \dots, 36 \end{aligned} \quad (41)$$

The same X locations are used to calculate grid points on the upper and lower surfaces. The lift coefficient derived for this point distribution is 21% less than the analytical thin wing solution, because there are not enough points in the proximity of the leading edge to follow the strong variations. In order to attract more grid points toward the leading edge ($X = -0.5$) the basic distribution from equation (41) is modified by the following equation.

$$X = (X^* - 0.5)^n - 0.5 \quad (42)$$

Aerodynamic coefficients derived for grid distributions that are obtained by equation (42) for $n = 2$ and $n = 3$, are given in Table 4. The results in Table III indicate that the lift coefficient is over-estimated by 10% ($n = 3$) and 5% ($n = 2$). The over-estimation is due to relatively large intervals in the mid chord vicinity and toward the trailing edge.

TABLE 4. Calculated Aerodynamic Coefficients for 10° Angle of Attack for Different Airfoil Grid Point Distribution

	C_L	C_m	ψ_{body}	Kutta Error
Basic	0.869	-0.0675	-0.22983	0.52×10^{-5}
$n = 2$	1.160	-0.00188	-0.22913	0.66×10^{-7}
$n = 3$	1.217	-0.00450	-0.23484	0.11×10^{-7}
Final	1.150	-0.00224	-0.22816	0.48×10^{-7}
Thin Wing Theory	1.096	0.0	-	

For a flat plate the analytical solution shows that $\sim 40\%$ of the lift is generated by the 0.1 chord length from the leading edge (Appendix B).

This suggests that 40% of the points should be in this interval, and this can be achieved by using equation (42) for $n = 2$. Thus, the final point distribution employs equation (42) for the 29 points that fall within the 0.1 chord length, and the remaining points are distributed by 10 linearly increasing intervals between 0.1 and 0.5 chord length and equal intervals from mid-chord toward the trailing edge (Table 4). The final airfoil representation over-estimates the thin wing theory by only 4.5%. It seems reasonable to assume that a finer grid will provide a better correlation.

The pressure coefficient is derived from the stream function solution using equation (31). As the trailing edge is a re-entrant point, the pressure coefficient is calculated twice for this point; once as a point on the lower surface, and second as a point on the upper surface, using one sided difference expressions. Because of residual errors in the calculations, slightly different values are obtained in violation of Kutta condition. The mismatch is resolved by interpolating the value on the lower surface using sixth order Lagrange interpolation and substituting the same value to the upper surface point. Fig 17 shows a typical chord-wise variation of pressure coefficient.

Lift and quarter chord moment coefficients are obtained by integrating pressure coefficient (Equations (32) and (33)). For an ideal symmetric airfoil, the quarter chord moment coefficient is zero and a non-zero calculated moment coefficient is a measure to the error introduced in pressure coefficient. The calculated coefficients are shown in Table 5 and a plot of lift coefficient variation with angle of attack is in Fig 18. The figure shows a very reasonable 5% correlation between thin wing theory and finite difference results.

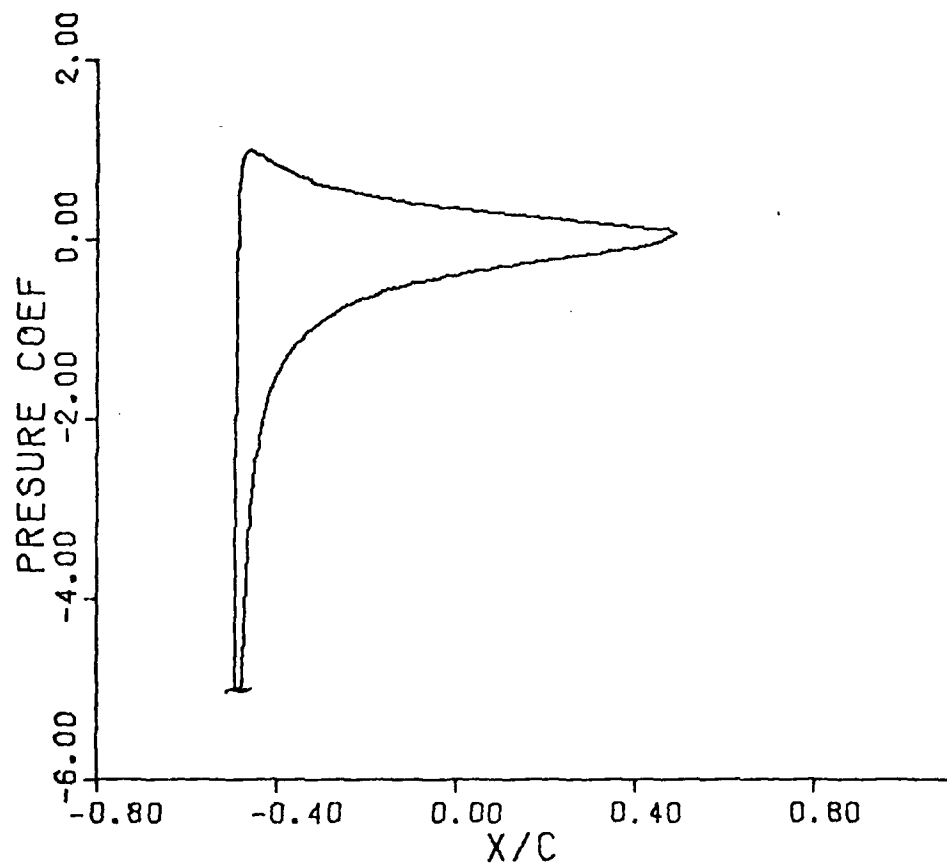


FIGURE 17. Pressure Coefficient vs. Nondimensionalized Chord Length in Free Stream Direction (Typical for Thin Airfoil).

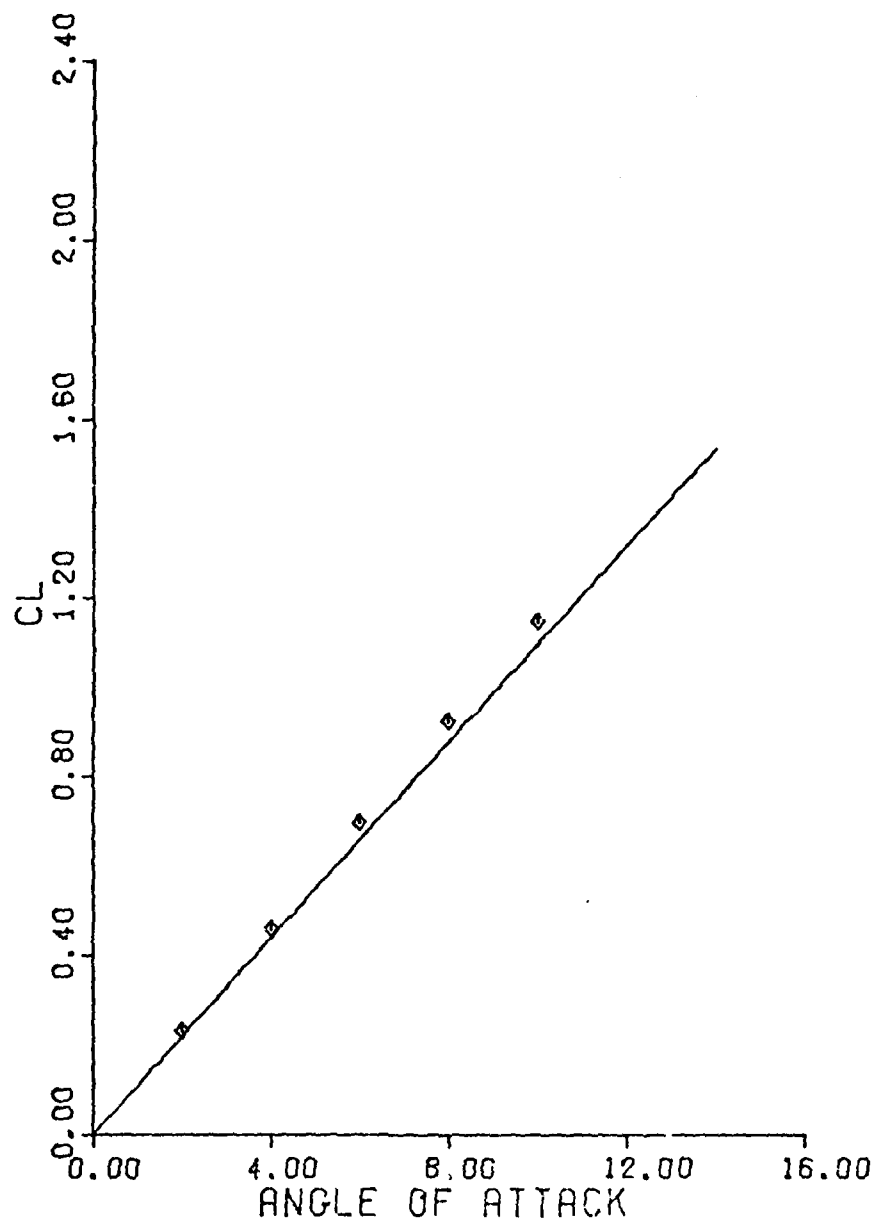


FIGURE 18. Free Stream Lift Coefficient vs. Angle of Attack

— Finite Singularity Method

◊ Finite Difference Method

TABLE 5. Aerodynamic Coefficients for Free Stream as Function of Angle of Attack - Finite Difference Method

α	C_L	$C_{mc}/4$	ψ body.	Kutta Error
2	0.230	-0.31×10^{-4}	-0.04512	0.161×10^{-3}
4	0.460	-0.37×10^{-4}	-0.09018	0.421×10^{-3}
6	0.696	-0.17×10^{-2}	-0.13719	0.220×10^{-3}
8	0.924	-0.21×10^{-2}	-0.18277	0.140×10^{-4}
10	1.150	-0.22×10^{-2}	-0.22817	0.483×10^{-5}

TABLE 6. Aerodynamic Coefficients in Ground Effect as Function of Ground Distance and Angle of Attack - Finite Difference Method

α	G.D.	C_L	$C_{mc}/4$	body	Kutta Error
10	0.25	1.379	-0.355×10^{-1}	-0.110	0.207×10^{-6}
10	0.50	1.123	-0.825×10^{-2}	-0.133	0.222×10^{-7}
10	0.75	1.190	-0.415×10^{-2}	-0.152	0.195×10^{-6}
10	1.00	1.162	-0.107×10^{-2}	-0.165	0.660×10^{-7}
10	1.50	1.142	-0.483×10^{-3}	-0.185	0.366×10^{-6}
4	0.25	0.644	-0.199×10^{-1}	-0.0475	0.237×10^{-6}
4	0.50	0.539	-0.825×10^{-2}	-0.0565	0.242×10^{-7}
4	0.75	0.500	-0.366×10^{-2}	-0.0622	0.386×10^{-9}
4	1.00	0.479	-0.212×10^{-2}	-0.0672	0.274×10^{-7}
4	1.50	0.466	-0.147×10^{-2}	-0.0746	0.203×10^{-6}

Airfoil in Ground Effect

For the ground effect solution the same airfoil type and airfoil body point distribution are used. The outer boundary is of rectangular shape in which the base is the ground and the top and sides are at "infinity" (ten chord units). Half of the outer boundary points (36) are on the ground base with linearly increasing intervals from the mid-base toward the sides (Table 7). The point at the outer boundary at the same ξ as the trailing edge is on the base about 20% of the distance from the mid-base toward the right side. This location is picked to get a physical coordinate system that remains nonsingular around the trailing edge (Figs 19 and 20). The initial guess for the transformation is equally spaced intervals in each direction with special attention to the region between the airfoil and the ground where each guess has a gradually decreasing slope changing from angle of attack to zero.

The stream function equation is solved by the same Kutta condition iteration procedure, as before. The outer boundary and initial guess values are of a uniform flow at zero angle of attack. The C_L and $C_{m_{c/4}}$ variations with ground distance for 4 and 10 degrees angle of attack are given in Table 6 and in Figures 21 and 22 where they are compared against finite singularity results. It is noted that a much better correlation is achieved for 4 degrees angle of attack than for 10 degrees. The mismatch can be explained by noting that finite singularity method is based on thin wing theory that is limited to small angles of attack and hence to small lift coefficients. Another point of comparison between finite singularity method and finite difference stream function solution arises from comparing the variation of ground velocity (Fig 23) where good correlation is obtained.

Summary

In this chapter airfoil flow field solution is obtained for the stream function equation for potential flow. Here, the stream function equation is solved by finite difference techniques on a body fitted coordinate system. A linear interpolation scheme is developed to satisfy the Kutta flow condition at the trailing edge. A criterion for grid point distribution over the airfoil is established. To resolve the strong leading edge gradients, 40% of the grid point must be distributed over 0.1 chord length about the leading edge. Variation of C_ℓ and $C_{m_{a.c.}}$ with angle of attack and ground distance agree well to the variation derived from finite singularity method (Chapter II).

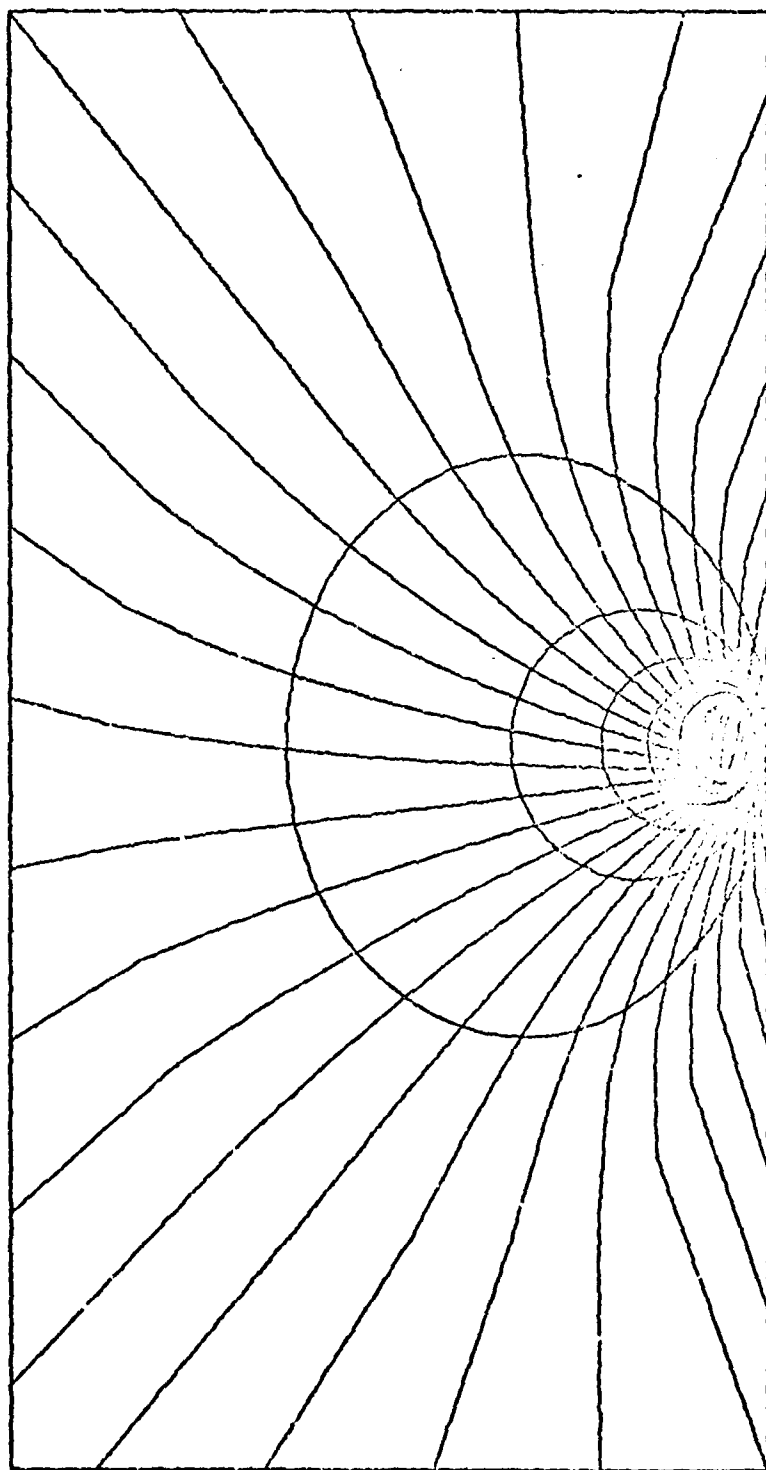


FIGURE 19. Body-Fitted Coordinate System for Airfoil in Ground Effect
Each second ξ line and each fifth η line are shown.

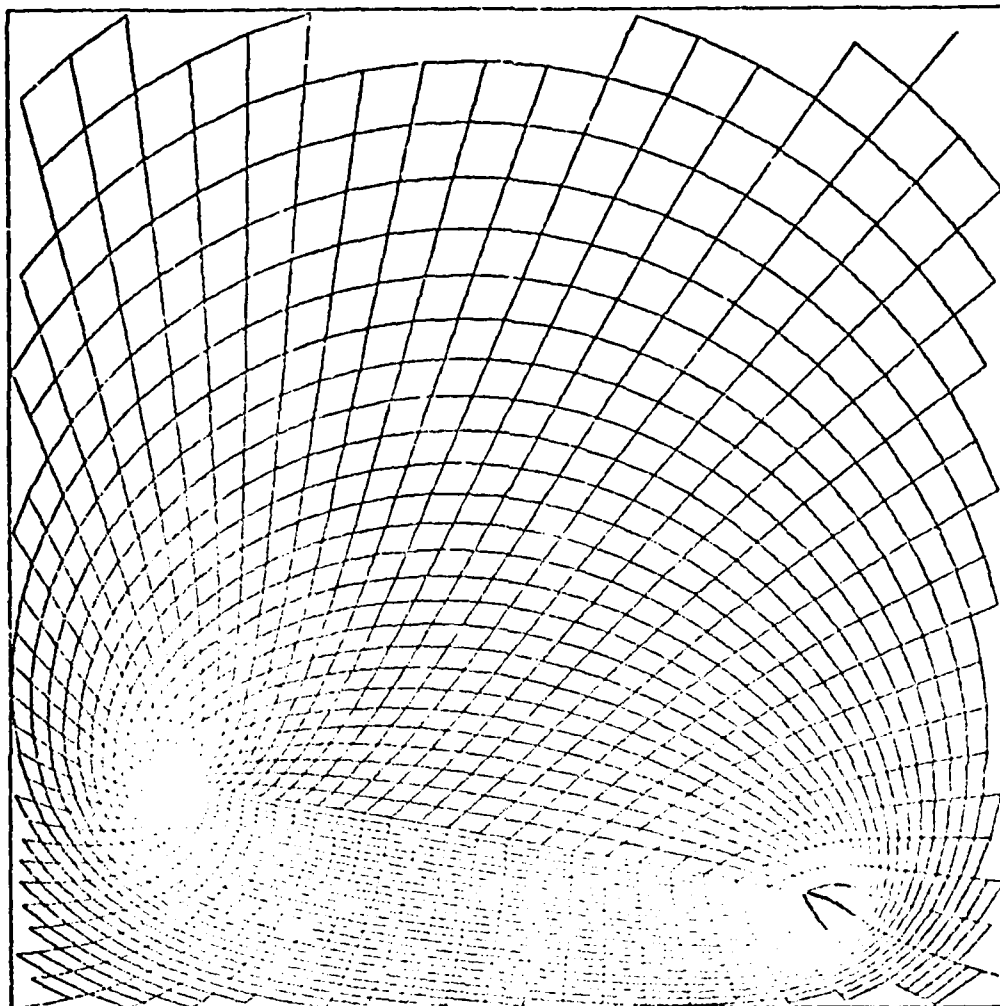


FIGURE 20. Body-Fitted Coordinate System for Airfoil in Ground Effect, Partial Region

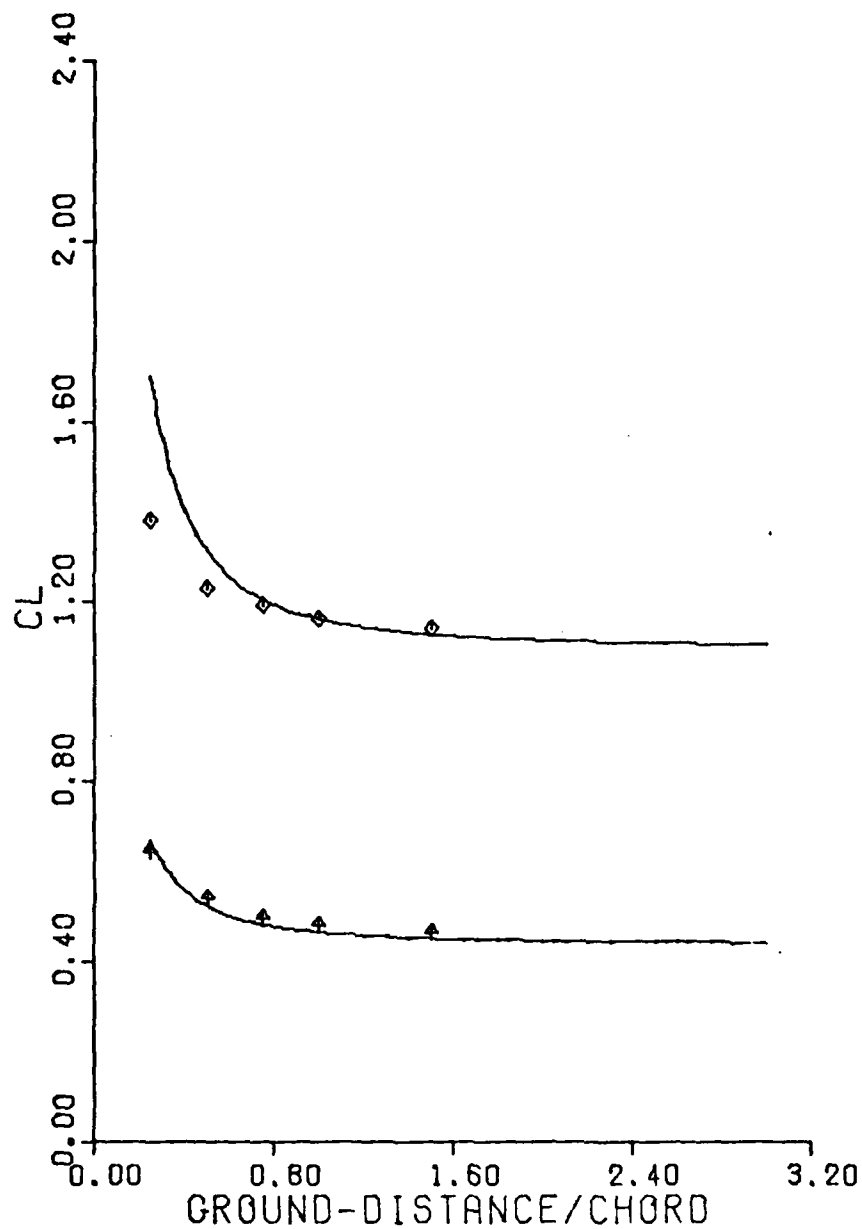


FIGURE 21. Lift Coefficient vs. Ground Distance, Angle of Attack as a Parameter (Finite Difference Method).

- - Finite Singularity Method
- △ - Finite Difference Method - 4°
- ◇ - Finite Difference Method - 10°

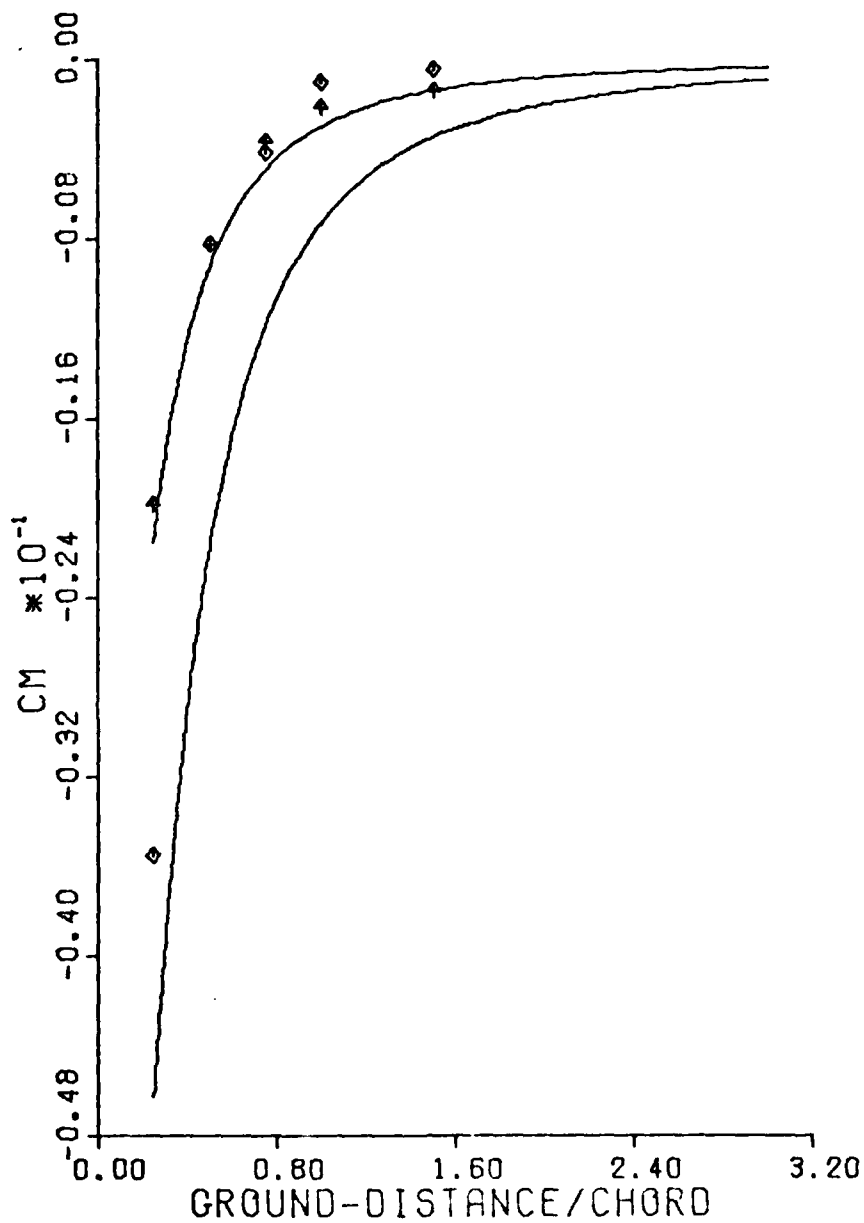


FIGURE 22. Quarter-Chord Moment Coefficient vs. Ground Distance. Angle of Attack as a Parameter (Finite Difference Method).

- - Finite Singularity Method
- ◊ - Finite Difference Method - 10°
- △ - Finite Difference Method - 4°

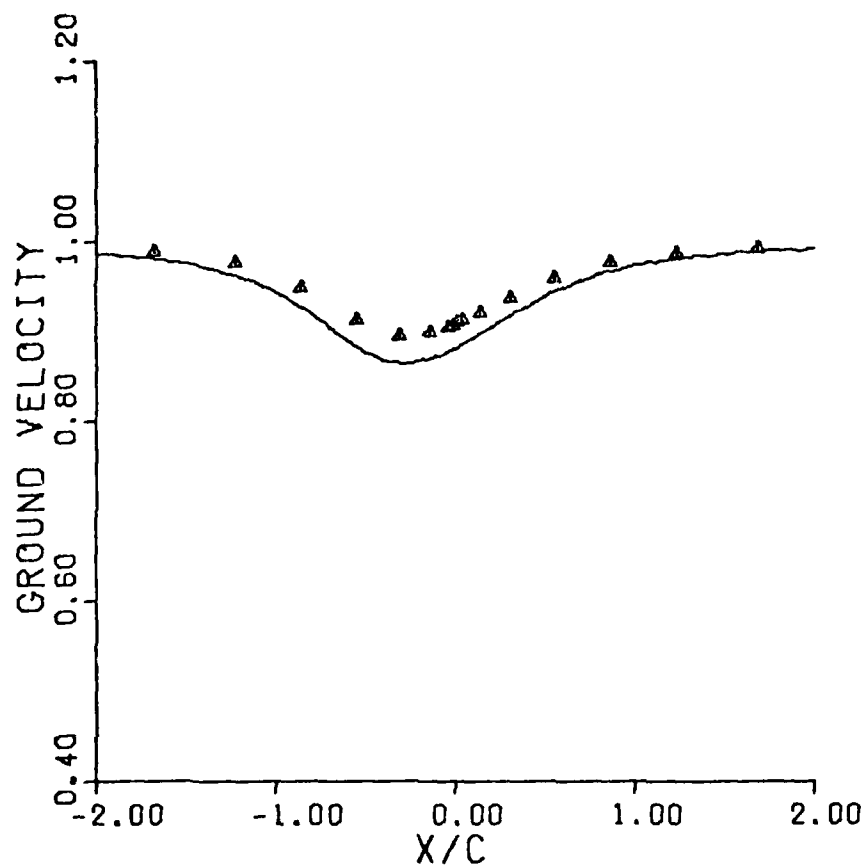


FIGURE 23. Ground Velocity vs. Nondimensionalized Length
in Free Stream Direction.
(4°-Angle of Attack, 0.5-Ground Distance)
- Finite Singularity Method
Δ Finite Difference Method

TABLE 7. Numerical Data for Rectangular Outer
Boundary for Airfoil in Ground Effect

POINT	X	Y	POINT	X	Y
1	2.1987	-.5000	37	-8.8235	10.0000
2	1.6812	-.5000	38	-7.6471	10.0000
3	1.2335	-.5000	39	-6.4706	10.0000
4	.8557	-.5000	40	-5.2941	10.0000
5	.5477	-.5000	41	-4.1176	10.0000
6	.3096	-.5000	42	-2.9412	10.0000
7	.1413	-.5000	43	-1.7647	10.0000
8	.0429	-.5000	44	-.5882	10.0000
9	.0143	-.5000	45	.5882	10.0000
10	-.0143	-.5000	46	1.7647	10.0000
11	-.0429	-.5000	47	2.9412	10.0000
12	-.1413	-.5000	48	4.1176	10.0000
13	-.3096	-.5000	49	5.2941	10.0000
14	-.5477	-.5000	50	6.4706	10.0000
15	-.8557	-.5000	51	7.6471	10.0000
16	-1.2335	-.5000	52	8.8235	10.0000
17	-1.6812	-.5000	53	10.0000	10.0000
18	-2.1987	-.5000	54	10.0000	8.8333
19	-2.7861	-.5000	55	10.0000	7.6667
20	-3.4434	-.5000	56	10.0000	6.5000
21	-4.1705	-.5000	57	10.0000	5.3333
22	-4.9674	-.5000	58	10.0000	4.1667
23	-5.8342	-.5000	59	10.0000	3.0000
24	-6.7709	-.5000	60	10.0000	1.8333
25	-7.7774	-.5000	61	10.0000	.6667
26	-8.8538	-.5000	62	10.0000	-.5000
27	-10.0000	-.5000	63	8.8538	-.5000
28	-10.0000	-.5000	64	7.7774	-.5000
29	-10.0000	1.8333	65	6.7709	-.5000
30	-10.0000	3.0000	66	5.8342	-.5000
31	-10.0000	4.1667	67	4.9674	-.5000
32	-10.0000	5.3333	68	4.1705	-.5000
33	-10.0000	6.5000	69	3.4434	-.5000
34	-10.0000	7.6667	70	2.7861	-.5000
35	-10.0000	8.8333	71	2.1987	-.5000
36	-10.0000	10.0000			

VI. HOVERCRAFT STREAM FUNCTION SOLUTION

The hovercraft discussion is limited to the fundamental case of symmetric hovering, although asymmetric configurations are also feasible. The purpose is to emphasize the difference between this case and airfoil stream function solution and suggest appropriate solutions to get a well defined jet.

Hovercraft Model

The peripheral jet type hovercraft for this 2-D model is a rectangle of 0.9×0.1 units with two 0.1 diameters semi-circular ends (Fig 24). The two peripheral jets are 0.1 units width and are located symmetrically near the rectangle ends. The body point distribution for hovercraft numerical definition assures enough points to resolve both the two semi-circular ends and the peripheral jets in particular (Table 8). The outer boundary is a rectangle in which the base is the ground.

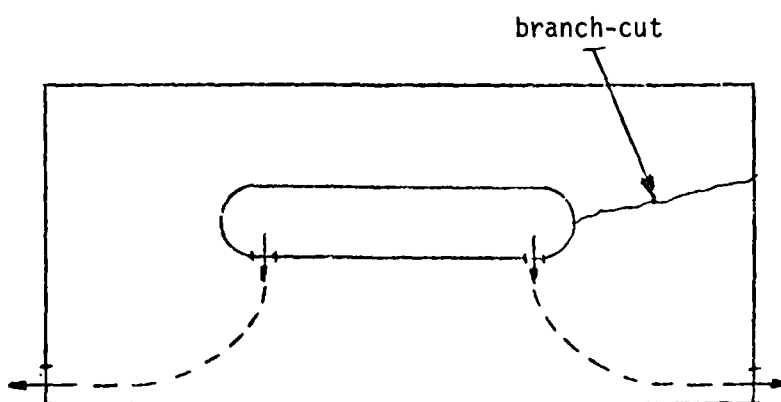


Figure 24. Hovercraft Model

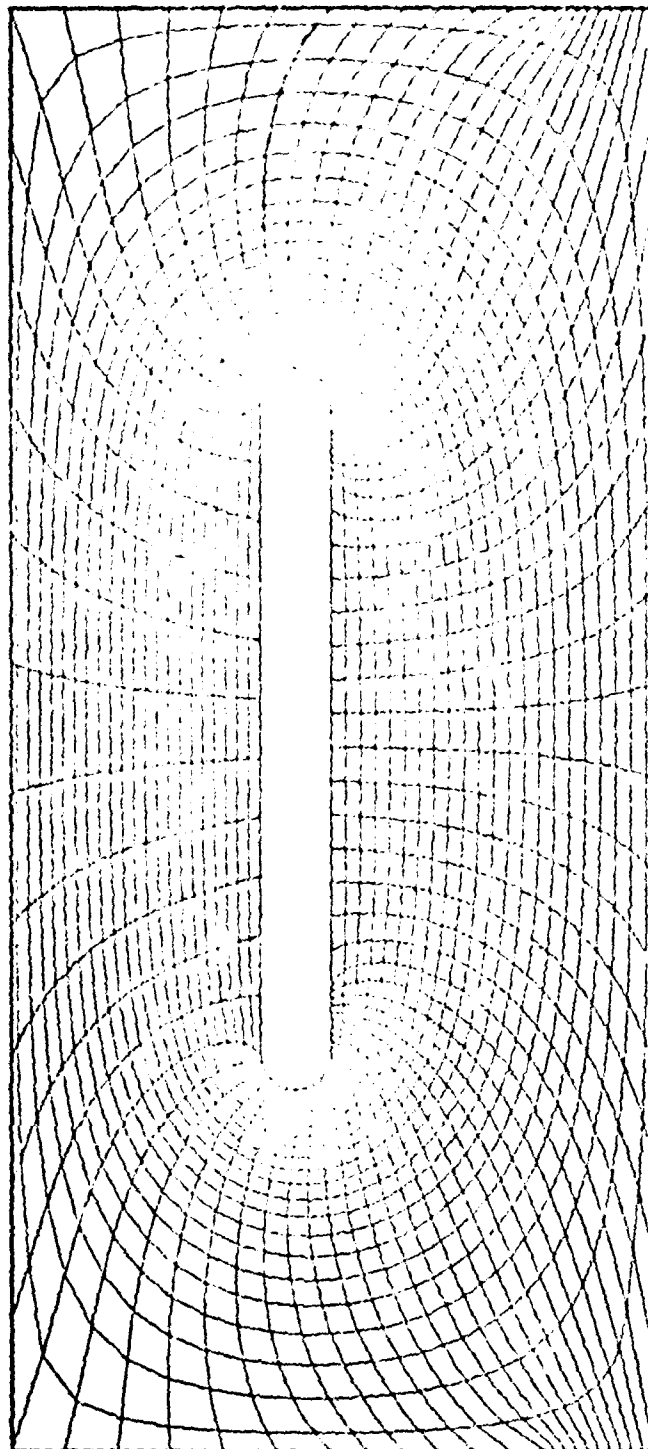


Figure 25. Body Fitted Coordinate System for Hovercraft in Ground Effect

TABLE 8. Numerical Data for a Hovercraft Model

POINT	X	Y	POINT	X	Y
1	.5000	0.0000	37	-.4000	-.0500
2	.4983	-.0129	38	-.4100	-.0500
3	.4933	-.0250	39	-.4200	-.0500
4	.4854	-.0354	40	-.4300	-.0500
5	.4750	-.0433	41	-.4400	-.0500
6	.4629	-.0483	42	-.4500	-.0500
7	.4500	-.0500	43	-.4629	-.0483
8	.4400	-.0500	44	-.4750	-.0433
9	.4300	-.0500	45	-.4854	-.0354
10	.4200	-.0500	46	-.4933	-.0250
11	.4100	-.0500	47	-.4983	-.0129
12	.4000	-.0500	48	-.5000	0.0000
13	.3900	-.0500	49	-.4983	.0129
14	.3800	-.0500	50	-.4933	.0250
15	.3700	-.0500	51	-.4854	.0354
16	.3600	-.0500	52	-.4750	.0433
17	.3500	-.0500	53	-.4629	.0483
18	.3403	-.0500	54	-.4500	.0500
19	.3267	-.0500	55	-.3602	.0500
20	.2100	-.0500	56	-.2064	.0500
21	.1633	-.0500	57	-.2045	.0500
22	.1167	-.0500	58	-.1227	.0500
23	.0700	-.0500	59	-.0409	.0500
24	.0233	-.0500	60	.0409	.0500
25	-.0233	-.0500	61	.1227	.0500
26	-.0700	-.0500	62	.2015	.0500
27	-.1167	-.0500	63	.2864	.0500
28	-.1633	-.0500	64	.3682	.0500
29	-.2100	-.0500	65	.4500	.0500
30	-.2567	-.0500	66	.4629	.0483
31	-.3033	-.0500	67	.4750	.0433
32	-.3500	-.0500	68	.4854	.0354
33	-.3600	-.0500	69	.4933	.0250
34	-.3700	-.0500	70	.4983	.0129
35	-.3800	-.0500	71	.5000	0.0000
36	-.3900	-.0500			

TABLE 9. Numerical Data for Outer Boundary for Hovercraft

POINT	X	Y	POINT	X	Y
1	1.0000	-.0500	37	-1.0000	-.4250
2	1.0000	-.1000	38	-1.0000	-.4100
3	1.0000	-.1500	39	-1.0000	-.3950
4	1.0000	-.2000	40	-1.0000	-.3800
5	1.0000	-.2500	41	-1.0000	-.3650
6	1.0000	-.3000	42	-1.0000	-.3500
7	1.0000	-.3500	43	-1.0000	-.3300
8	1.0000	-.3650	44	-1.0000	-.2500
9	1.0000	-.3800	45	-1.0000	-.2000
10	1.0000	-.3950	46	-1.0000	-.1500
11	1.0000	-.4100	47	-1.0000	-.1000
12	1.0000	-.4250	48	-1.0000	-.0500
13	1.0000	-.4400	49	-1.0000	.0250
14	1.0000	-.4550	50	-1.0000	.1000
15	1.0000	-.4700	51	-1.0000	.1750
16	1.0000	-.4850	52	-1.0000	.2500
17	1.0000	-.5000	53	-1.0000	.3250
18	.8667	-.5000	54	-1.0000	.4000
19	.7233	-.5000	55	-.8182	.4000
20	.6000	-.5000	56	-.6364	.4000
21	.4667	-.5000	57	-.4545	.4000
22	.3333	-.5000	58	-.2727	.4000
23	.2000	-.5000	59	-.0909	.4000
24	.0667	-.5000	60	.0909	.4000
25	-.0667	-.5000	61	.2727	.4000
26	-.2000	-.5000	62	.4545	.4000
27	-.3333	-.5000	63	.6364	.4000
28	-.4667	-.5000	64	.8182	.4000
29	-.6000	-.5000	65	1.0000	.4000
30	-.7333	-.5000	66	1.0000	.3250
31	-.8667	-.5000	67	1.0000	.2500
32	-1.0000	-.5000	68	1.0000	.1750
33	-1.0000	-.4850	69	1.0000	.1000
34	-1.0000	-.4700	70	1.0000	.0250
35	-1.0000	-.4550	71	1.0000	-.0500
36	1.0000	-.4400			

The point collection for outer boundary definition assures good resolution for the jet outlets (Table 9). To obtain a reasonable-looking boundary fitted coordinate system in the peripheral jet region with the limited size arrays, the outer boundary sides and top are as shown (Fig 25). The initial guess is rectangles with equally spaced intervals in each direction.

Multi-valued Stream Function

Peripheral jets introduce the same problem for a stream function solution as a fluid source, for which integration of transverse velocities along any closed path around the source results in two stream function values at the same point. The difference between the two stream function values is proportional to the source strength, which will be referred as $\Delta\psi$. The stream function solution can be made single-valued by choosing a branch cut along an arbitrary line connecting the inner and outer boundaries. Stream lines values change by an amount $\Delta\psi$ as they cross the branch cut. Explicit difference equation (36) remains valid for irrotational flow for every point in the field except those which form differences across the branch cut. For the points on the branch cut the difference equation is

$$\begin{aligned} \psi_{i,j} = & \tilde{\alpha}_{i,j}(\psi_{i-1,j} + \Delta\psi + \psi_{i+1,j}) - \tilde{\beta}_{i,j}(-\psi_{i-1,j+1} + \psi_{i+1,j+1} + \psi_{i-1,j-1} - \psi_{i+1,j-1}) \\ & + \tilde{\gamma}_{i,j}(\psi_{i,j-1} + \psi_{i,j+1}) + \tilde{\delta}_{i,j}(-\psi_{i,j-1} + \psi_{i,j+1}) + \tilde{\tau}_{i,j}(-\psi_{i-1,j} - \Delta\psi - \psi_{i+1,j}) \end{aligned} \quad (43)$$

The explicit difference expression (Equations (36) and (43)) are solved for the computational field with Dirichlet type boundary conditions. The jets are assumed to be uniform flow at the nozzles and at the outlets,

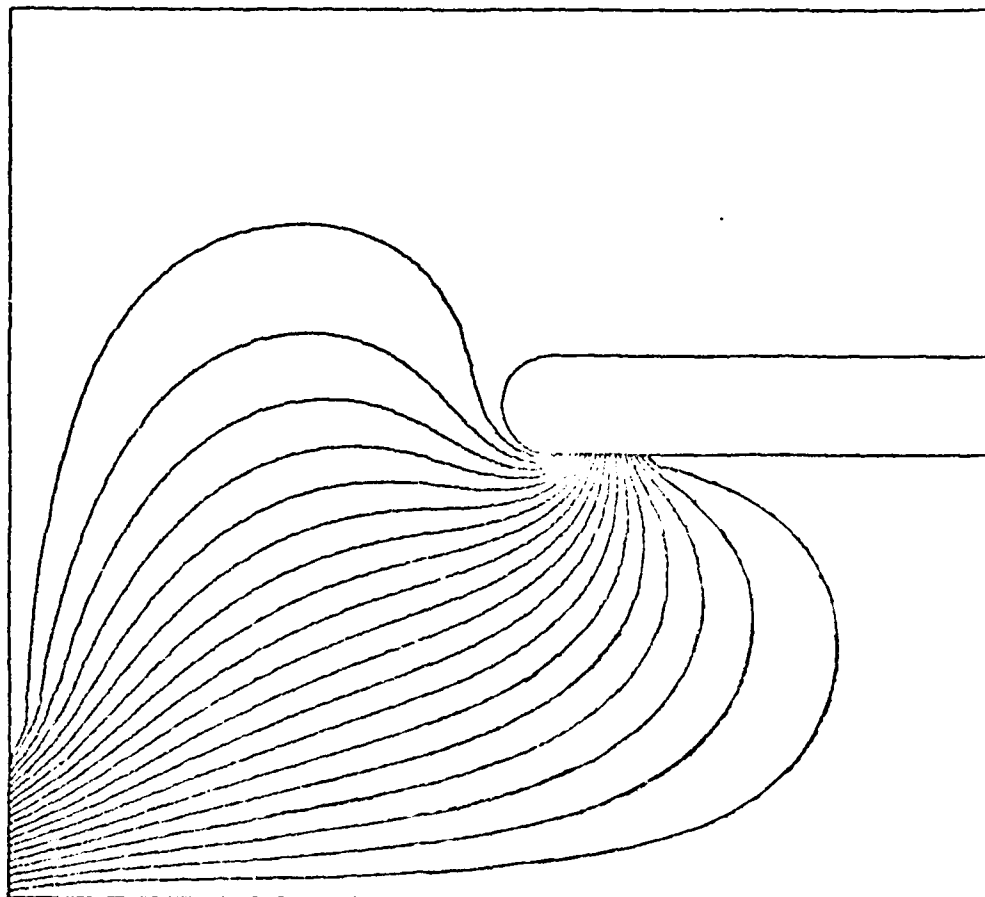


Figure 26. Stream Function Contour Plot for Hovercraft, Potential Flow Solution

with an assumed velocity at the nozzles. Stream function values are calculated by integrating the velocities where the ground and hovercraft base between the jets are assigned to be zero. A contour plot for the stream function is shown in Fig 26, from which it may be concluded that solving an irrotational flow does not provide a solution with a well-defined jet even though the stream function is single valued.

Vorticity

In order to obtain a better defined jet, vorticity is introduced in two shear layers on the jet boundaries. Vorticity in the flow field changes the governing equation to Poisson type.

$$\Delta^2 \psi = -\omega \quad (44)$$

For simplicity the vorticity will be calculated as function of the stream function by assuming an arbitrary velocity profile across the jet as shown in Fig 27. The chosen velocity profile is uniform velocity across the center semi-width tapering linearly toward the boundaries.

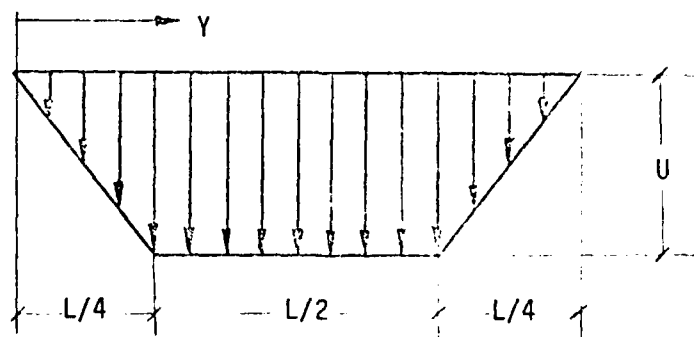


Figure 27. Jet Velocity Profile

The total change of stream function value across the jet is

$$\psi^* = 3 UL/4 \quad (45)$$

Stream function variation as function of Y .

$$\begin{aligned} \psi &= 2 UL(Y/L)^2 & 0 < Y/L < 1/4 \\ &UL/8 + UL(Y/L - 1/4) & 1/4 < Y/L < 3/4 \\ &3 UL/4 - 2 UL(Y/L - 1)^2 & 3/4 < Y/L < 1 \end{aligned} \quad (46)$$

Vorticity is calculated from equation (44).

$$\begin{aligned} \omega &= -\nabla^2 \psi = -4U/L & 0 < Y/L < 1/4 \\ &0 & 1/4 < Y/L < 3/4 \\ &+4U/L & 3/4 < Y/L < 1 \end{aligned} \quad (47)$$

Equation (47) can be written in a more convenient form as:

$$\begin{aligned} \omega &= -\nabla^2 \psi = -4U/L & 0 < \psi/\psi^* < 1/6 \\ &0 & 1/6 < \psi/\psi^* < 5/6 \\ &+4U/L & 5/6 < \psi/\psi^* < 1 \end{aligned} \quad (48)$$

Equation (48) expresses vorticity as a function of stream function only and thus is a very convenient form. The explicit difference expression corresponding to equation (44) is:

$$\psi_{i,j} = (\text{R.H.S. of equation 43}) + [J_{i,j}^2 / 2(\alpha_{i,j} + \gamma_{i,j})] \cdot \omega(\psi_{i,j}) \quad (49)$$

Equation (49), which includes vorticity and a branch cut, together with Dirichlet boundary condition as described above, produced a well defined jet (Fig 28).

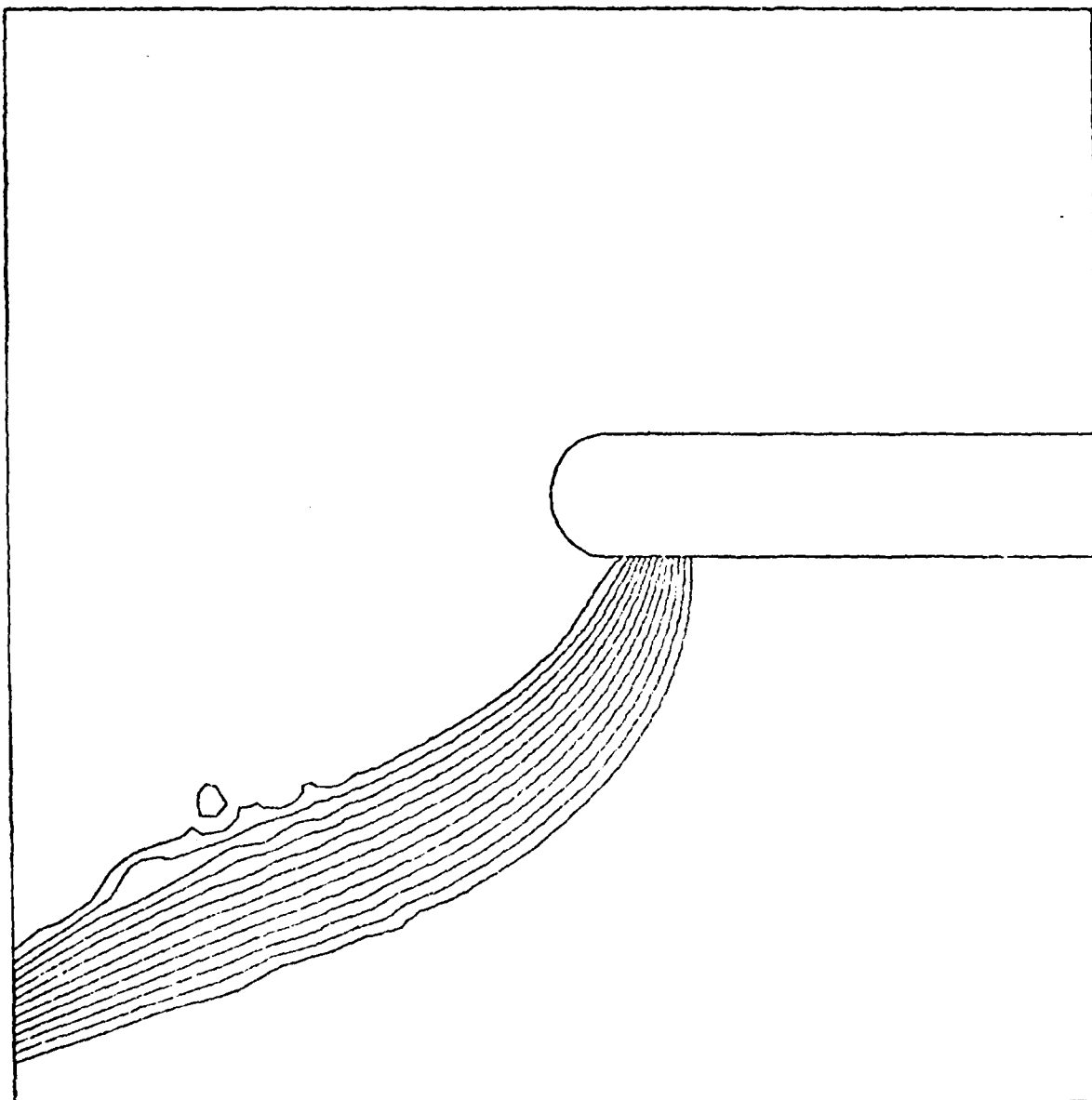


Figure 28. Stream Function Contour Plot for Hovercraft,
Vorticity in Jet Edges

Pressure Derivation

Cushion pressure is a very important parameter for hovercrafts. Exponential theory, the commonly used analytical method for cushion pressure calculations (Ref 3), assumes that the jet between the nozzle and the ground forms a section of a torrus. All the other analytical methods have to assume the jet geometry as well. Actual jet geometry variation from the analytical model result in inaccuracy in cushion pressure calculated.

A finite difference method, rather than assuming jet geometry, solves for it by using the stream function solution. The pressure field can be obtained by the Poisson equation (Ref 6).

$$\nabla^2 P = 2 \left[\left(\frac{\partial^2 \psi}{\partial x^2} \right) \left(\frac{\partial^2 \psi}{\partial y^2} \right) - \left(\frac{\partial^2 \psi}{\partial x \partial y} \right)^2 \right] \quad (50)$$

Equation (50) is usually solved with Neuman type boundary condition that can be determined by Euler equations on the boundary. This suggested approach for pressure field calculation has not been tried as part of this study, and is left for further investigation.

Summary

In this chapter the 2-D flow field for an air cushion vehicle with peripheral jet is obtained from the stream function-vorticity, Poisson equations. As this case introduces a flow source within the computational field and, thus, raises a question of a multivalued stream function, a branch cut is introduced. Solution of an irrotational flow field shows that the jet spreads widely. In order to obtain a better defined jet, vorticity is derived from an arbitrary assumed velocity distribution at

the jet outlets and assumed to be constant along stream lines. The investigation must be continued to determine the influence of the above assumptions on the pressure field.

VII. CONCLUSIONS

Stream function-vorticity equations expressed in numerical finite difference formulation can be used on a body fitted coordinate system to obtain flow field for both an airfoil varying degrees of ground effect and air cushioned vehicle with a peripheral jet. The airfoil flow field is solved for the potential flow case. For lift and quarter-chord moment coefficients at various angles of attack and ground distances, good agreement is observed between independent solutions with a finite difference method and a finite singularity method. A criterion for grid points distribution about the leading edge is set up to resolve the strong gradients in this region properly. The stream function-vorticity equation is solved with branch cut needed for fluid sources in the hovercraft. To obtain a well defined jet, vorticity in the edges of jets is essential and can be simply modeled with some success.

Several aspects remain to be investigated to complete the feasibility determination. The first major aspect is to develop a stable formulation to obtain the pressure field from the stream function field by solving the Poisson equation with appropriate boundary conditions. This appears straightforward. Also, pressure field sensitivity to both assumed jet vorticity distribution and vorticity transport, must be evaluated.

The results of this work indicate that a 2-D stream function-vorticity solution to an air cushioned airfoil appears feasible. If results remain positive after last questions are answered, the result will be a powerful analytical tool for flow field analysis.

BIBLIOGRAPHY

1. Karamcheti, K. Principles of Ideal-Fluid Aerodynamics. New York: John Wiley and Sons, 1966.
2. Bisplinghoff, R.L., and H. Ashley and R.L. Halfman. Aeroelasticity. Reading, Massachusetts: Addison-Wesley Publishing Company, 1957.
3. Elsley, G.H. and A.J. Devereux. Hovercraft Design and Construction. Cambridge, Maryland: Cornell Maritime Press, 1968.
4. Thompson, J.F. and F.C. Thames and W.C. Mastin. Boundary Fitted Curvilinear Coordinate Systems for Solution of Partial Differential Equations on Fields Containing Any Number of Arbitrary Two Dimensional Bodies. NASA CR-2729.
5. Abbott, I.H. and A.E. VonDolnhoff. Theory of Wing Sections. New York: McGraw Hill Book Company.
6. Roach, P.J. Computational Fluid Dynamics. Albuquerque, New Mexico: Hermosa Publishers.
7. Mantle, P.J. A Technical Summary of Air Cushion Craft Development. Report Number: DTNSRDC 4727.

APPENDIX A

COMPUTER PROGRAMS DESCRIPTION

Appendix A contains short descriptions on the computer programs that are used. Only the five main programs are discussed; other short programs that are used are not of special interest. Four out of those five programs were basically written by the AF Flight Dynamics Laboratory, Wright-Patterson AFB, but were changed to accommodate for the special needs of this study. The main objective of each program is:

1. Program CORDMN - Generation of boundary fitted coordinate system.
2. Program ABGMN - Derivation of transformation parameters $(\alpha, \beta, \gamma, \sigma, \tau, J)$.
3. Program PSIMN - Stream function field solution.
4. Program UVP - Derivation of velocity components and pressure fields.
5. Program AERDCO - Derivation of aerodynamic coefficients.

The structure of the programs and some input and output information is described for each program separately.

Program CORDMN

This program generates 2-D body fitted coordinate system for any arbitrary number of bodies in the region. Input data consists of inner boundary and optionally the outer boundary (if not generated by the program), max number of grid points in each direction in the transformed

plane, number of bodies in the field, max number of iterations, acceleration parameters, allowable X and Y errors, various header lines, print and plot control parameters. Optionally the field generated by a previous run may be read in instead of the boundaries. Output data consists of X and Y arrays that may be printed out and/or written on disk (tape 10).

Subroutine BNDRY:	Produces an outer boundary if not given by input data.
Subroutine GUESSA:	Produces an initial guess for the entire computational field.
Subroutine TRANS:	SOR iteration routine for field solution (X,Y).
Subroutine RHS or RHSBL:	Assigns coefficient for exponential series that are the right hand side of transformation equations. Subroutine RHS is an exponential decay right hand side where subroutine RHSBL coefficients are derived from Blasius flat plate boundary layer solution.
Function ERROR:	Calculates largest field error between two consecutive iteration steps.
Subroutine SLEQ:	Simultaneous solution of linear algebraic equation used to derive RHSBL coefficients.
Subroutine MAXMIN:	Calculates the maximum and minimum values of a two dimensional array. Used for plots scaling.
Subroutine REED:	Reads data from disks.
Subroutine WRITDK:	Writes on disk and prints output data.
Subroutine CORPLT:	Plots first guess and final coordinate system.

Program ABGMN

This program calculates numerically (second order difference expressions) the transformation parameters for the coordinate system arrays (X,Y) that were produced by program CORDMN. It should be noted that the calculations give 4α , 4β , 4γ , $4J$, 2α , 2τ , and not the transformation parameters themselves. Input data consists of X and Y arrays that are read from disk (tape 10), control parameter for sharp trailing edge, control parameter for sharp trailing edge, control parameter for body transformation, parameters change, and various print parameters. Output data is written on disks (tape 11 - 4α , 4β , 4γ ; tape 12 - $4J$; tape 13 - 2α , 2τ).

- Subroutine ABGJ: Calculates the transformation parameters by second order difference expressions.
- Subroutine INOUT: Controls data input and output.
- Subroutine CHNG: Calculates the expression α/J and γ/J for $J = 1$ (on the body) and stores the values as β and γ on the body (note that β and γ on the body are not used for stream function field solution).
- Subroutine TEDGE: Recalculates transformation parameters using central differencing if the body does not have sharp trailing edge.
- Subroutine MAXMIN: Calculates the maximum and minimum values of a two dimensional array. Used for plots scaling.
- Subroutine REED: Reads data from disks.
- Subroutine WRITDK: Writes on disk and prints output data.

Program PSIMN

This program produces a stream function field solution by solving explicit numerical expressions. Input data consists of coordinate system given by X and Y arrays (tape 10), transformation parameters (Tapes 11 and 13), max number of iterations, convergence criterion, angle of attack, free stream velocity, Kutta convergence criterion, max number of Kutta iterations, stream function value on the body, and print control parameters. For hovercraft solution jets velocity is given as input. Output data consists of stream function field array (tape 14) and body pressure coefficient one dimensional array (tape 16).

Subroutine BNDRYP:	Produces outer boundary condition.
Subroutine GUESSP:	Produces stream functional initial guess.
Subroutine COEFS:	Produces new coefficients needed by stream function numerical expression.
Subroutine LAPSOR:	Produces field solution.
Subroutine PRES:	Calculates pressure coefficient by Bernoulli equation.
Function ERROR:	Calculates largest field error between two consecutive iteration steps.
Subroutine REED:	Reads data from disks.
Subroutine WRITDK:	Writes on disk and prints output data.
Subroutine KUTTA:	Calculates body stream function slope at the trailing edge to compare against camber slope (airfoil only).
Subroutine OMEGA:	Calculates vorticity values a function of stream function values.

Program UVP

This program produces velocity components and invicid pressure fields. Input data consists of coordinate systems given by X and Y arrays (tape 10), stream function field array (tape 14), angle of attack, velocity at infinite to reference velocity ratio, control parameter to choose between 2-D and axisymmetric case and print control parameter. Output data consists of u and v velocity components and pressure fields (tape 20).

Subroutine VEL: Produces velocity component field by numerical differentiation of stream function field.

Subroutine CPINV: Produces pressure field for invicid flow by Bernoulli's equation.

Subroutine REED: Reads data from disks.

Subroutine WRITDK: Writes on disk and prints output data.

Program AEROCO

This program calculates lift and moment coefficients for an airfoil in invicid flow field by Bernoulli equation. Input data consist of coordinate system given by X and Y arrays (tape 10), pressure coefficient on the body (tape 16), and angle of attack. Output data consist of pressure coefficient printout and lift and moment coefficients.

Subroutine CLCM: Calculates lift and moment coefficients by integrating numerically pressure coefficient by Simpson's one third rule.

Subroutine LAGINT: Corrects pressure coefficient at the trailing edge by using Lagrange interpolation formula.

Subroutine WRIPR: Writes on disk and prints single dimensional array output data.

APPENDIX B

Chord-Wise Cp Variation for Flat Plate

Appendix B contains an analytical analysis for chord-wise Cp variation for a flat plate. The analysis is done using thin wing theory vortices distribution for a flat plate (Ref 1). The form of the derived results is percentage of lift coefficient vs. non-dimensionalized chord length from the leading-edge. The results are used as a measure for point distribution on the airfoil that will pick up the high gradients around the leading edge without amplifying Cp values on the rear section of the airfoil.

Lift coefficient is calculated by integration of vorticity distribution, which leads to the following:

$$\theta = \arccos (2 x/c-1) \quad (B-1)$$

$$\%C_l = 100 [1-(\theta-\sin\theta)/\pi] \quad (B-2)$$

the results from B-1 and B-2 are given in Table B-1 and Figure B-1. Results show that 40% of the lift for a flat plate is generated by 10% of chord from the leading edge, and only 18% of the lift is generated by the semi-chord between mid-chord and trailing edge. Conclusion from the lift contribution by various parts of the airfoil is that very rapid pressure changes and, hence, velocity changes occur in the vicinity of the leading edge. In the finite difference numerical field solution where the matrices sizes are tried to be kept reasonable, more points should be put near the leading edge to pick up those changes. The chosen point distribution, that show to give good results, was 40% of the points within 10% from the leading edge and only 27% of the point on the rear semi-chord.

Table B-1. Percent of C_l vs. Nondimensional Chord
Measured from Leading Edge

x/c	% C_l	x/c	% C_l
0.	0.	0.10	39.6
0.01	12.7	0.20	55.0
0.02	17.9	0.30	66.1
0.03	21.9	0.40	74.8
0.04	25.3	0.50	81.8
0.05	28.2	0.60	87.6
0.06	30.9	0.70	92.3
0.07	33.3	0.80	95.9
0.08	35.5	0.90	98.6
0.09	37.6	1.00	100.0

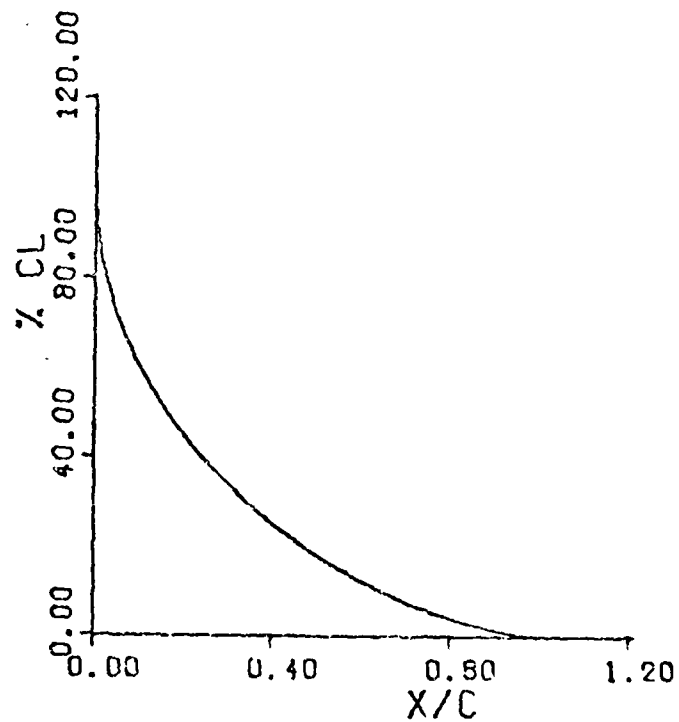


Figure B-1. Graphic Presentation of Table B-1

VITA

Itzhak Dvir was [REDACTED]. He completed his high school [REDACTED] in 1965. He studied in the "Technion" in Haifa, Israel through the ROTC program, and graduated with a Bachelor of Science Degree in Aeronautical Engineering in 1969. He joined the Israel Air Force in November 1969 and was assigned to Air Force Headquarters, Research and Development Department, Aeronautical Design Branch. In this assignment he was responsible for designing and monitoring aircraft modifications. In June 1977 he entered the Air Force Institute of Technology for the Graduate Aeronautical Engineering program. He is married to [REDACTED], and a [REDACTED].

[PII Redacted]

Permanent Address: [REDACTED]

This thesis was typed by [REDACTED]

[PII Redacted]

UNCLASSIFIED

SECURITY CLASSIFICATION OF THIS PAGE (When Data Entered)

REPORT DOCUMENTATION PAGE		READ INSTRUCTIONS BEFORE COMPLETING FORM
1. REPORT NUMBER	2. GOVT ACCESSION NO.	3. RECIPIENT'S CATALOG NUMBER
AFIT/GAE/AA/78D-6		
4. TITLE (and Subtitle)		5. TYPE OF REPORT & PERIOD COVERED
2-D Flow Numerical Solution for Airfoil and Hovercraft in Ground Effect		M.S. Thesis
		6. PERFORMING ORG. REPORT NUMBER
7. AUTHOR(s)		8. CONTRACT OR GRANT NUMBER(s)
Itzhak Dvir Major IAF		
9. PERFORMING ORGANIZATION NAME AND ADDRESS		10. PROGRAM ELEMENT, PROJECT, TASK AREA & WORK UNIT NUMBERS
Air Force Institute of Technology (AFIT/EN) Wright-Patterson AFB, Ohio 45433		
11. CONTROLLING OFFICE NAME AND ADDRESS		12. REPORT DATE
		December 1978
		13. NUMBER OF PAGES
		84
14. MONITORING AGENCY NAME & ADDRESS (if different from Controlling Office)		15. SECURITY CLASS. (of this report)
Air Force Flight Dynamics Laboratory (AFFDL) Wright-Patterson AFB, Ohio 45433		UNCLASSIFIED
		15a. DECLASSIFICATION DOWNGRADING SCHEDULE
16. DISTRIBUTION STATEMENT (of this Report)		
Approved for public release; distribution unlimited		
17. DISTRIBUTION STATEMENT (of the abstract entered in Block 20, if different from Report)		
18. SUPPLEMENTARY NOTES		
Approved for public release; distribution unlimited IAW AFR 190-17		
JOSEPH P. HIPPS, Major, USAF Director of Information		
19. KEY WORDS (Continue on reverse side if necessary and identify by block number)		
Air Cushioned Vehicle Hovercraft Wing in Ground Effect		
20. ABSTRACT (Continue on reverse side if necessary and identify by block number)		
A proposal has been made to compute a 2-D numerical solution to the stream function - vorticity equation to analyze the flow field, both of an airfoil in ground effect and of an air cushion vehicle of arbitrary geometry supported by peripheral jets. This report is an investigation of both problems. Finite difference solutions of the stream function-vorticity equation are computed on a body fitted coordinate system. The Laplace equation for streamlines around an airfoil in ground effect is solved, and results are compared to an analytic		

DD FORM 1473

EDITION OF 1 NOV 65 IS OBSOLETE

UNCLASSIFIED

SECURITY CLASSIFICATION OF THIS PAGE (When Data Entered)

UNCLASSIFIED

SECURITY CLASSIFICATION OF THIS PAGE(When Data Entered)

finite singularity solution. Comparison of C_L and $C_{ma.c}$ at varying angles of attack and ground distance indicate good agreement. The finite difference method is found to be sensitive to grid point distribution about the leading edge, for which a criterion is established. Since an air cushion vehicle acts as a flow source within the field, the finite difference expression is modified to accommodate a branch cut. The presence of vorticity is essential to definition of the peripheral jets. The vorticity distribution, derived from arbitrary velocity distribution at jet outlets and assumed to be constant along streamlines, leads to a stable solution of the stream function-vorticity equation.

UNCLASSIFIED

SECURITY CLASSIFICATION OF THIS PAGE(When Data Entered)